Understanding the Profitability Potential of Ancillary Service Markets: Techno-Economic Analysis of a Hybrid Power Plant

Charles Alexander Stark

Thesis to obtain the Master of Science Degree in

Energy Engineering and Management

Supervisors: Prof. Luís Filipe Moreira Mendes
Dr. Rafael Eduardo Guédez Mata

Examination Committee

Chairperson: Prof. José Manuel Costa Dias de Figueiredo
Supervisor: Prof. Luís Filipe Moreira Mendes
Member of the Committee: Prof. Luís António Fialho Marcelino Ferreira

November 2017

Acknowledgements

First and foremost, I would like to express my sincere gratitude to my technical supervisor Dr. Rafael Guedez. He and I were originally paired up via a mentorship program run by my master's program (InnoEnergy) and during the course of that relationship he assisted me in finding my thesis topic. As a supervisor, Rafael gave me immense guidance, advice and support throughout the entire lifespan of my thesis project. In addition to Dr. Guedez, I want to thank Dr. Filipe Mendes who acted as my thesis supervisor at IST in Lisbon. Filipe gave me immensely helpful feedback and guidance as I navigated the final stages of my report and he ensured that I delivered a quality product that I would be proud of. I would also like to say thank you to Dr. Monika Topel and Monica Arnaudo, both of whom took time out of their busy schedules to help me troubleshoot problems and find solutions which greatly aided my progress.

Next, it is important that state my appreciation of Luis Castillo, who acted as my contact and advisor on behalf of Lark Energy. Luis went to great lengths to ensure that I had all the information necessary in order to carry out this work. He also made sure to frequently meet with me so that we could preserve continuous communications as progress was made.

To my friend, Kevin Larchet, I owe a great deal of thanks. Kevin had performed a similar thesis to me in the previous year and had helped to develop some of the software I was using. There were several occasions in which I had a doubt about how to perform a certain function with the software and Kevin always sought to help point me in the right direction.

I would be remiss if I didn't exhibit my immense gratitude to my family, both my parents, Tom and Debbie, and my sister, Chelsea. From the first moment when I told them that I was quitting my job and moving to Europe to study Renewable Energy Engineering, my family has shown me nothing but support, love and encouragement. I can safely say that I wouldn't be in the position I am today without them, and knowing that they believe in me gives me confidence moving forward.

Lastly, I want to express my thanks to all the friends at KTH that I made during the six months I was there. There are too many names to list them all here, but I am happy to say that the friendship and camaraderie I found with all of them I was a driving force that helped me to push through tough days of grinding away on this thesis.

Resumo

O principal objetivo do presente trabalho foi o de realizar uma análise termo-económica de uma central híbrida para fornecer três mercados distintos (energia elétrica, regulação de frequência e capacidade instalada) no Reino Unido, determinando-se a melhor configuração de três tecnologias: solar fotovoltaica, baterias e gerador a gás natural. Com este objetivo, foram analisadas múltiplas configurações utilizando-se uma ferramenta de otimização de sistemas energéticos. Para tornar isto possível o software foi modificado desenvolvendo-se novas rotinas para expandir as suas funcionalidades. Os principais parâmetros que foram comparados para cada configuração foram o investimento de capital (CAPEX), o preço de oferta necessário para o fornecimento de serviços de regulação da frequência da rede (FFR *Fee*) e as emissões de carbono. Os resultados mostram que um sistema baterias-gerador com 20 MW de geradores e com 5 MWh de armazenamento com baterias são a melhor combinação de CAPEX ((\$11.05 mil) e FFR *Fee* (63.22 \$/h). O CAPEX desta solução é 34% menor que o de um sistema constituído por 8 MW de geradores e 20 MWh de armazenamento com baterias e é 71% menor que o de um sistema com 32.5 MWh de armazenamento em baterias. O FFR *Fee* é 23% menor que o de um sistema fotovoltaico-baterias-geradores. No entanto, uma análise de sensibilidade baseada em previsões da evolução dos mercados mostrou que outras soluções poderiam acabar por se tornarem melhores e que a escolha de uma configuração que possa evoluir com o tempo é provavelmente a melhor decisão.

Palavras-chave: análise termo-económica, mercados da energia, otimização, armazenamento com baterias

Abstract

This thesis project's goal is to perform a techno-economic analysis of a hybrid power plant participating in three separate markets (wholesale electricity, firm frequency response, and capacity) in the United Kingdom, seeking to determine the optimal configuration of technologies and the plant's required market tender fee. To achieve this, multiple configurations of three main technologies (solar photovoltaic cells, batteries, and natural gas-fired generators) were analyzed using an energy system optimization tool. To make this possible, the software had to be modified by developing new scripts to increase its functionality, which would enable it to provide an optimal case for each of the four configurations under consideration. The main factors that were compared between each plant were their capital expenditure (CAPEX) value, the tender price required for providing frequency response services (FFR Fee), and carbon emissions. Results showed that a Battery-Generator plant with 20 MW of generators and 5 MWh of battery storage provided the optimal combination of CAPEX (\$11.05 mil) and FFR Fee (63.22 \$/hr), since the CAPEX was 34% lower than for a Battery-Generator plant consisting of 8 MW of generators and 20 MWh of battery storage, the FFR FEE was 23% lower than a photovoltaic-battery-generator

plant, and the CAPEX was 71% lower than for a 32.5 MWh battery stand-alone plant. However, a sensitivity analysis based on predicted market trends found that other solutions could be superior and that choosing a configuration that can evolve with time would be wise.

Keywords: techno-economic analysis, energy markets, optimization, battery storage

Contents

List of Tables

List of Figures

Nomenclature

Greek Symbols

η	efficiency [%]
ω	Angular velocity [rad/s]

Energy

kWh	kilowatt hour
MWh	megawatt hour
GWh	gigawatt hour

Power

Wp	watt produced
kW	kilowatt
MW	megawatt
GW	gigawatt
GWp	gigawatt produced

Chemical Abbreviations

CO_2	Carbon dioxide
HSO_4	Hydrogen sulfide
Mg	Magnesium
Pb	Lead
PbO_2	Lead-oxide
$PbSO_4$	Lead sulfate (lead acid)
Sb	Antimony

V^{2+}	Vanadium
VO_2^+	Dioxovanadium
VO^{2+}	Vanadium oxide

Equation Symbols

A	Area of solar module $[m^2]$
f	Frequency [Hz]
FF	Fill factor [-]
I	Cell current [A]
I_0	Reverse saturation current [A]
I_{mo}	Moment of Inertia [kg-m^2]
I_{MP}	Maximum power point current [A]
I_s	Source current [A]
I_{sc}	Short circuit current [A]
k	Boltzmann constant [J//K]
KE	Kinetic Energy [J]
m	Modified ideality factor [-]
P_{MP}	Maximum power point [W]
P_{plant}	nominal power of the PV plant that the PV plant can generate [MW]
$P_{pv-meas}$	measured PV power [MW]
q	charge [C]
$Q_{rem}(t)$	Normalized remaining battery capacity in period t
$SOC^*(t)$	Setpoint for the state of charge of the battery [%]
SOC_{chrg}	Sum of the percentage gained in all the timesteps in which the battery was charging [%]
SOC_{diff}	Difference in the state of charge between one timestep and the next [%]
SOC_{dis}	Sum of the percentage lost in all the timesteps in which the battery was discharging [%]
t	Time period [h]

T	Temperature [K]
$TE(t)$	Total processed energy (from start to period t)
UF	Utilization factor of the battery
V_{MP}	maximum power point voltage [V]
V_{oc}	Open circuit voltage [V]
v_T	Temperature voltage [V]

Glossary

AC Alternating Current

BESS Battery Energy Storage System

BOP Balance of Plant

BOS Balance of Systems

Cont Contingency

Conv Converter

CAPEX Capital Expenditure

CM Capacity Market

DC Direct Current

DOD Depth of Discharge

DYESOPT Dynamic Energy System Optimizer

EOL End of Life

ECS Electronics Control System

FFR Firm Frequency Response

Gen Natural gas-fired generator

HES Hybrid Energy System

Inv Inverter

IRR Internal Rate of Return

KPI Key Performance Indicators

LCOE Levelized Cost of Electricity

MATLAB Matrix Laboratory

NOH Normal Operating Hours

NPC Net Present Cost

NPV Net Present Value

OFGEM Office of Gas and Electricity Markets

OPEX Operating Expenditure

PCS Power Conditioning System

PV Photovoltaic solar energy

SOC State of Charge

Soft Soft Costs

TRNSYS Transient Systems Simulation Program

TSO Transmission System Operator

USD Dollars ($)

VRFB Vandium Redox Flow Battery

WACC Weighted Average Cost of Capital

Chapter 1

Introduction

1.1 Motivation

As the year 2020 draws closer, countries in Europe strengthen their push toward Horizon 2020 and a lower carbon future by investing in renewable energy production technologies. In certain countries, the electricity mix in the grid is starting to be taken over by electricity generated from renewable energy sources (i.e. solar power, wind power, and hydro power). In some cases, whole countries are running on 100% renewable energy for short periods of time, as was the case for 4 straight days in Portugal in 2016 [1]. All of this is positive news and means that things are heading in the right direction, but there are still some looming problems that need solving. One of the main issues that needs to be addressed moving forward pertains the intermittency of renewables. An unexpected cloud can pass overhead and constrict the production of a solar photovoltaic (PV) plant for several minutes. Similarly, a drastic variation in wind speed, in either direction, can reduce the output of a wind park or temporarily halt their production, full stop.

Due to the variability of electricity production sources feeding into a grid, fluctuations are expected. Small fluctuations are commonplace and do not require reactionary measures. Large fluctuations, however, are less frequent but far more detrimental to equipment performance and grid stability. A large variation in the frequency can cause instability in the rotational speed of a grid-connected turbine which leads to potentially damaging vibrations in the blades (a closer look at the reasons for this is provided in section 2.5.1) [2]. This issue has given rise to the requisite of having Firm Frequency Response (FFR) plants in place that are capable of rapidly coming online and generating electricity when the production from other sources drops off. In order to ensure that a system fault or blackout doesn't occur, these plants must respond to an event within 10 seconds of its occurrence [3].

Services like FFR do a great job of ensuring that current electricity generation is not in jeopardy, however in an effort to plan ahead and guarantee that

their systems won't encounter any issues in the years to come, countries have begun to enact a new device known as a Capacity Market (CM). The in-depth details of how CMs function will be addressed in section 2.6.2.3, yet the general idea is that each country's grid transmission operator (TSO) reaches agreements with plants four years ahead of time to so that they can be certain that there will be enough future installed capacity to meet their demand projections. The United Kingdom launched its Capacity Market in 2014, and it is going to start paying plants for their generating capacity in the coming year (2018) [4].

From the perspective of energy project developers in the UK, the FFR and CM markets are just a few of many avenues to supplement the revenue generation of a newly built or yet to be constructed plant. Revenue supplementation, going above the simply generating and selling electricity to the grid, has become necessary so that the project developers and plant operators can ensure a project's profitability, and thus, it's viability. This need stems from the fact that over the past decade the U.K., along with many other developed countries around the globe, has seen a drop off in the overall energy and electricity demand led by the introduction of new, energy-efficient technologies along with higher industry standards for efficiency [5, 6].

Thus, in recent years, in an effort to combat the decrease in demand and the increase in competition, developers have started offering their generation services in a variety of ways (e.g. FFR tenders). This sets up the central idea of the work that was performed hereunder: under the current multi-market conditions present in the U.K., what type of hybrid plant (technology and capacity-wise) should a developer seek to build that will both satisfy technical requirements while being financially optimal?

The answer to this question was particularly interesting to one of the main project partners that assisted in the completion of this work. This partner being Lark Energy, a developer and maintainer of commercial and utility scale energy projects, ranging from solar farms to biomass to natural gas-powered generators, which aims to provide its customers with cleaner, reliable solutions that meet their energy needs. As a means of helping to narrow the scope of the project, Lark provided a list of specifications based on their current capabilities and desired business strategy. They also laid out some assumptions that could be made in order to alleviate a lack of information in certain areas.

Lark Criteria

- Plant shall participate in three separate markets: Electricity Market, Frequency Response Market, and Capacity Market

- Plant shall consist of one of or a combination of the following technologies:

    - Solar Photovoltaic Modules

    - Electrochemical Batteries

    - Natural Gas-fired Generators

- Plant shall consist of no more than 20MW of installed capacity from each individual technology

- With regards to the FFR market, the plant shall be able to provide both primary and secondary dynamic response services (to be explained in section 2.6.2.2)

- The plant configuration shall either minimize the investment costs or require the lowest possible compensation price for operating

Assumptions

- The design of the plant could be performed by utilizing historical market data for electricity prices and grid frequency values

- It could be assumed that any action which affects the Capacity Market will also equally affect the Frequency Response Market, so in essence they could be treated to be aligned. To elaborate, if an event occurs which forced the FFR market to require a reduction in plant production, the CM would be forced to make the same request.

The information listed above was used as boundary conditions so that a techno-economic analysis could be carried out which sought to find the most suitable answer to the research question on Lark's behalf.

1.2 Previous Works

Many works pertaining to the topics of battery and energy storage, revenue maximization, electrical grid regulation, and plant hybridization were reviewed. Journal entries and papers by Black et al. [7], Byrne et al. [8], Rasmussen et al. [9], Ortega-Vazquez et al. [10], Eto et al. [11], Mokrian et al. [12], Olatomiwa et al. [13], Baneshi et al. [14], and Tsuanyo et al. [15]. All of thesse shared aspects or ideas with this particular thesis work yet it was decided that only the most relevant works should be summarized in this report. The following three works are all thesis projects that served to aid in the further development of the DYESOPT software and, in part, provided groundwork that would be used in this project. DYESOPT is a simulation tool that was originally developed by Dr. Rafael Guedez and his research partners in the Energy Department of KTH in Stockholm, and since it's development many students and researchers have helped to expand its functionality (the tool is explained in greater detail in section 3.1).

1. "Techno-economic Analysis of Combined Hybrid Concentrating Solar and Photovoltaic Power Plants: A Case Study for Optimizing Solar Energy Integration into the South African Electricity Grid", by Castillo, 2014.

3

(a) In this study, a techno-economic model was developed for both a CSP and PV power plant, at which point a hybrid plant was constructed by combining the two models. It was the goal of the study to determine the optimal control strategy under varying scenarios in order to best assimilate this proposed plant into the South African electricity grid. The PV model developed by Castillo in his thesis is the same one that will be utilized in the work hereunder [16].

2. "Solar PV-CSP Hybridisation for Baseload Generation: A Techno-economic Analysis for the Chilean Market", by Larchet, 2015.

   (a) The goal of this master's thesis project was to analyze the viability of a CSP-PV hybrid plant with battery storage for an area with high irradiance levels in the Chilean desert. The work also performed a multi-objective pareto optimization, which focused on two different objective scenarios; a minimization of both LCOE and CAPEX, and alternatively, a minimization of both LCOE and the CO2 emissions generated by the plant. This not only required for adjustments to be made to the CSP and PV models already existing in DYESOPT, but in addition to that the creation of a techno-economic model for the BESS was needed [17].

3. "Impact of Time-of-Delivery Schemes on Optimum Solar Hybrid Power Plants: A Techno-Economic Study", by Hansson, 2016.

   (a) The main objective of this study was to investigate how modifying the time-of-delivery (TOD) schemes could make different hybrid solar power plants (CSP, CSP-PV and PV-BESS) achieve profitability targets in certain markets. This called for the creation of a dynamic dispatch strategy that used mixture of the electricity price and the number of forecasted peak sun hours remaining at any given moment in time to dictate dispatch decisions [18].

Additional Works

The next couple of works do not pertain to the DYESOPT software but instead to the overall research question that this project sought to answer.

1. "Maximizing the value electricity storage", by Staffel & Rustomji, 2016.

   (a) This research by Staffel and Rustomji seeks to answer a research question lying in the same vein as the work completed hereunder; how to obtain the most economic benefit out of an energy storage system (such as BESS). They are able to effectively prove that a battery system operator could triple their profits by choosing to offer energy reserve services in addition to performing arbitrage activities. Although this work does perform a techno-economic analysis of a BESS participating in many markets in an attempt to maximize

economic value, it doesn't consider the possibility of hybridizing the system to include another technology [19].

2. "Optimal operation of a CHP plant participating in the German electricity balancing and day-ahead spot market", by Kumbartzky, Schacht, Schulz, and Werners, 2017.

   (a) This journal entry seeks to validate the assertion that in order for a combined heat and power (CHP) plant to remain competitive and maximize its profits it needs to participate in multiple markets, including the day ahead spot electricity market and the balancing market. The researches successfully developed a multi-stochastic mixed integer linear programming model that carried out the optimization of the CHP plant and heat storage, while simultaneously generating bids for the two targeted markets. Despite its similarites in terms of multi-market participation and usage of one type of energy storage, this work is clearly different for the fact that they have chosen to focus on the CHP technology instead of PV, batteries and gas generators [20].

1.3 Objectives

The main objective of this work is to establish if a hybrid power plant consisting of photovoltaic solar modules, electrochemical batteries, and natural gas generators can feasibly participate in a multitude of electricity sales and services markets in the United Kingdom, and additionally, to determine the optimum configuration of said power plant. Pursuant to this main objective, the following sub objectives were created.

- Perform a extensive literature review in order to discover any previous works which share relevance with this works main objective. The literature review also should examine the current state of the technologies under consideration and investigate other hybridization schemes that have been studied.

- Study and gain familiarity with the two main pieces of software which are paramount to this thesis (DYESOPT and TRNSYS).

- Develop two new models in the DYESOPT tool; one for the combined battery and generator plant, and the other for a hybrid PV-BESS-Gen plant. Aside from any findings generated by this thesis report, this objective had great importance because it would help to bolster the research capabilites of the DYESOPT tool and could be used by researchers henceforth.

- Find the optimal combination (capacity-wise) of batteries, generators (and possibly PV, if it proves to be cheaper).

- Determine the optimal price to offer FFR services and then compare this with current market average to validate the proposed hybrid plant will be on par or better than its competition.

1.4 Methodology Overview and Thesis Organization

In order to effectively carry out this analysis this thesis will first examine the background information (see chapter 2) and current status of the key technologies being considered (i.e. solar photovoltaic modules: section 2.1, electrochemical batteries: section 2.2, and gas generators: section 2.3). Then an examination will be made into recent developments in hybridization schemes (section 2.4), the issue of frequency balancing (section 2.5), and how this pertains to the UK system (section 2.6).

Following the background information, the methodology which was applied to structure and carry out this analysis will be presented (chapter 3). This methodology centers around the KTH in-house techno-economic analysis software tool, DYESOPT (section 3.1). An introduction of DYESOPT will be made, along with the new combined Photovoltaic-Battery Energy Storage-Gas Generator system (PV-BESS-Gen) hybrid model and dispatch strategy that was developed (section 3.6). Next, the economic functions will be enumerated and explicated, highlighting any key performance indicators (KPI) that DYESOPT takes into consideration (section 3.7). Finally, the idea of multi-objective optimization will be laid out and explained, as well as which specific design variables and objectives were being considered for this analysis (section 3.8).

All of this leads into the presentation of the results that DYESOPT's analysis has yielded (chapter 4). The results of a multi-objective optimizations are considered; the two chosen objectives were to find the plant that can offer FFR services at the cheapest price and find the plant with a minimum amount of carbon dioxide (CO_2) emissions. A comparison will then be shown to assess how a PV-BESS-Gen system, a BESS-Gen, and a standalone battery bank system stack up against one another (section 4.2). Finally, the results of three different sensitivity analyses (natural gas price, battery price, and electricity price) are given which includes a bit of speculation regarding the direction of each one of these markets moving forward and how it stands to impact the proposed solutions (section 4.3).

6

Chapter 2

Background

This chapter looks to provide a clearer understanding of all the concepts and technologies that are under consideration in this report.

2.1 Solar Photovoltaics

This section gives an overview of the operational theory of PV cells, how their performance can be quantified, some of their major issues, what the state of the market is currently, and which PV module was selected for this project.

2.1.1 Operational Theory

The basic solar photovoltaic cell is made up of a p-n junction diode, which is produced by joining a p-type and n-type semiconductor region. The p-type region is a semiconductor (most commonly Silicon) that has been "doped" with acceptor impurities, which equates to another metal (e.g. Boron) that has one fewer valence electrons and thus can accept a free electron from the silicon. On the other hand, the n-type region is a semiconductor that was doped with donor impurities; donor metals (e.g. Phosphorus) are those which have one additional valence electron and because of it are able to give one to the silicon. When the p-n junction is formed, there is a difference in the concentration of electrons and holes (the term given to a vacated space made by an electron after it leaves) which results in movement of the two. Electrons from the n-type region diffuse into the p-type region, and the holes in the p-type region move to the n-type region. This movement results in the formation of an electric field [21].

The solar cell has inherent current-voltage (I(V)) characteristics that are defined by its cell structure, material properties, and the operating conditions. The following equation can be evaluated to determine the I(V) characteristics of a solar cell.

$$I = I_{SC} - I_{01} \left[\exp\left(\frac{qV}{kT} \right) - 1 \right] - I_{02} \left[\exp\left(\frac{qV}{2kT} \right) - 1 \right] \qquad (2.1)$$
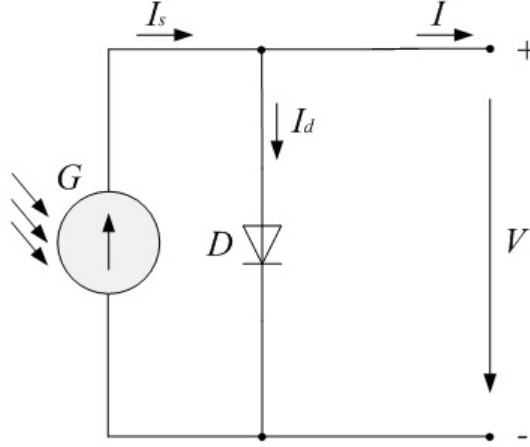
Figure 2.1: Depiction of an ideal model equivalent circuit for an illuminated solar PV cell [23]

In which Isc is the short circuit current, I_{01} is the dark saturation current due to recombination in the quasi neutral region, I_{02} is the dark saturation current due to recombination in the space-charge region, q is charge, V is voltage, T is temperature, and k is the Boltzman constant [22].

When the sun's rays reach the surface of the solar cell, the photon's energy creates free charge carriers. A solar cell under illuminated conditions can be represented by an equivalent circuit that consists of a diode (D) and a power source (see Figure 2.1). The power source (sun) generates a photo electric current (I_s) which has a direct correlation to the level of irradiance (G) [22]. It must be noted that this the simplest way to model a PV cell and although more accurate models exist it was decided to not modify the existing PV model which was already in place at the onset of the thesis work.

When analyzing a solar cell in the form of an equivalent circuit, there are a few very useful equations used to anticipate the cell's behavior. The first is the equation to find the cell current in the ideal model scenario (i.e. neglecting any losses due to shading or resistance, which will be addressed later).

$$I = I_s - I_0 \left[e^{\frac{V}{mV_T}} - 1 \right] \tag{2.2}$$

In which I_0 is the reverse saturation current, V is the voltage, m is the modified ideality factor and V_T is the temperature voltage [22]. Equation 2.2 is quite useful, as it can be rearranged in a variety of ways depending on the circumstance or input variables. In the open circuit condition, it takes the form of equation 2.3 which can then be rearranged to solve for the short circuit current (equation 2.4).

$$V_{oc} = mV_T ln\left(1 + \frac{I_{sc}}{I_0}\right) \tag{2.3}$$

$$I_{sc} = I_0\left(e^{\frac{V_{oc}}{mV_T}} - 1\right) \tag{2.4}$$

Where V_{oc} stands for the open-circuit voltage and I_{sc} represents the short circuit voltage [22]. Alternatively, the maximum power point current (IMP) can be found by inserting the maximum power point voltage (VMP) and using I_{sc} in place of I_s [22].

$$I_{MP} = I_{sc} - I_0\left(e^{\frac{V_{MP}}{mV_T}} - 1\right) \tag{2.5}$$

Rearranging once more yields an equation for V_{MP} [22].

$$V_{MP} = mV_T ln\left(1 + \frac{I_{sc} - I_{MP}}{I_0}\right) \tag{2.6}$$

Equations 2.7 and 2.8 show how to calculate V_T and m, resepctively [22].

$$V_T = \frac{kT}{q} \tag{2.7}$$

$$m = \frac{V_{MP} - V_{oc}}{V_T ln\left(1 - \frac{I_{MP}}{I_{sc}}\right)} \tag{2.8}$$

There are two big factors that affect the output power of a solar cell which have not yet been mentioned. These factors are the temperature and the irradiance level. Examining figures 2.2(a) and (b), it can be seen that as the irradiance level decreases and/or the temperature increases the maximum power diminishes.

2.1.2 Key Performance Metrics

The main figures of merit for a solar cell are I_{sc}, V_{oc}, V_{MP}, I_{MP}, along with the fill factor (FF) and the efficiency (η). The fill factor is defined in equation 2.9 [22]:

$$FF = \frac{V_{MP}I_{MP}}{V_{oc}I_{sc}} = \frac{P_{MP}}{V_{oc}I_{sc}} \tag{2.9}$$

Finally, the efficiency can be found by simply taking the ratio of maximum power point to incident power (see equation 2.10) [22].

$$\eta = \frac{P_{MP}}{P_{in}} = \frac{V_{oc}I_{sc}FF}{P_{in}} \tag{2.10}$$

An efficient solar cell will have a high I_{sc} value, a high V_{oc} value, and a FF value of close to one [22].
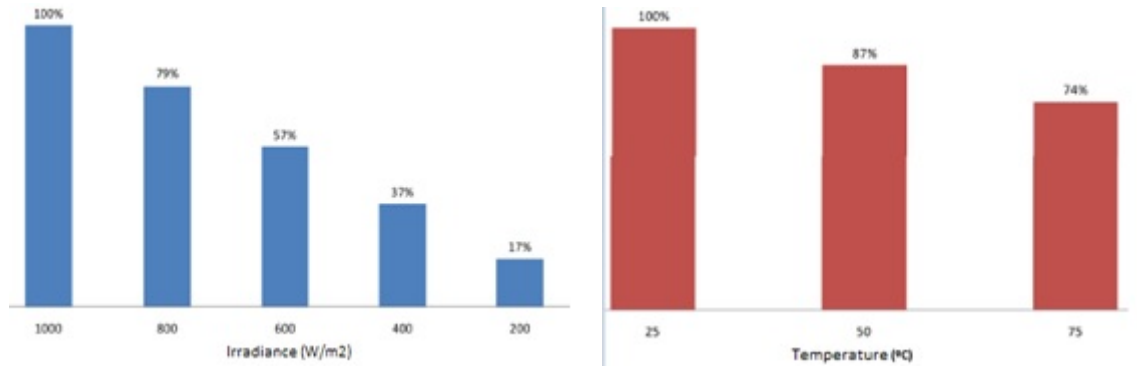
(a) Graph displaying the affect that different levels of irra-(b) Graph depicting the relationship between temperature and
diance has on the percent of maximum power produced   the percent of maximum power produced

Figure 2.2: Effects of irradiance and temperture on solar module output [22]
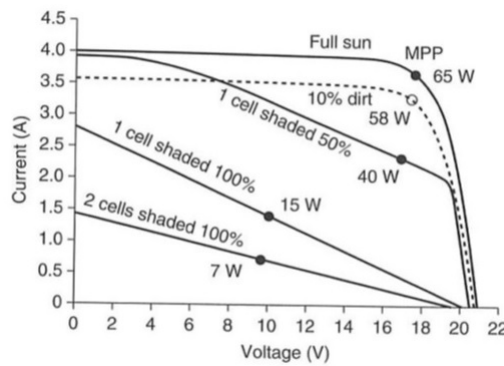
Figure 2.3: Effects of shading on the current and voltage of a 65W solar PV
module [22]

2.1.3   Issues

Shading

If even one cell in a module is shaded it can severely reduce the output power
of the module. As seen in figure 2.3, the power is reduced drastically when one
cell or two cells are fully shaded, and even shows a significant drop off when one
cell is only partially shaded.

Shading plays a large role in the design of a PV Plant with regards to spacing
considerations. One must ensure that the shadow from one row of modules is
not going to reach the row to either side during hours that have a lower solar
angle. This means that countries with limited space will not be able to install
expansive systems or will be forced to accept some production losses in the
morning and evening due to improper spacing.
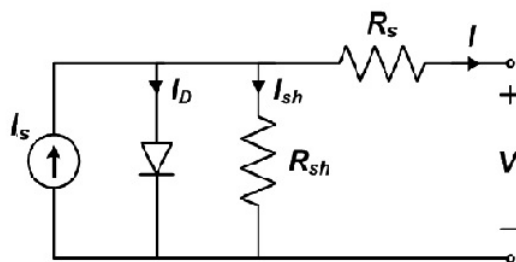
Figure 2.4: Equivalent circuit for a solar PV cell which includes series and shunt resistances [24]

Cleanliness

Figure 2.3 also illustrates another issue that PV modules typically have, which is they experience reduced efficiency when they are dirty. As the figure shows, the module in question is producing 58 W when only 10% dirty, as opposed to 65 W when clean (a reduction in power of 10.8%). A proactive effort must be made to ensure the cleanliness of the module surfaces is near optimal at all times in order to ensure the modules are generating their rated output.

Series and Shunt Resistances

Series and shunt resistance can limit the production of a PV module, however their effects are not taken into account by the model, leaving an in-depth overview unnecessary to the understanding of this thesis. However figure 2.4 has been provided to help provide a basic understanding of the concept.

Series resistance (R_s) is created by the contact resistance of wire leads and resistance of the semiconductor in the solar cells. Shunt resistance (R_{sh}) is created when the electric current finds an alternative path to take rather than flowing through the diode; this condition usually arises from manufacturing defects and the effects have shown to be more severe under low light conditions [22].

2.1.4 Current Market Trends

The capacity of solar PV has seen colossal growth over the past decade. In 2006, the total global installed generating capacity of PV was just north of 6 GW, whereas in 2015 that capacity had grown to over 219 GW, an increase of 3650% [25]. This growth has continued to accelerate and as of January 2017, the current global installed capacity was 310 GWp, and it is expected that in the next 4 years the cumulative global capacity will double again [26]. The solar PV market experienced an increase of 50% capacity in 2016, up to roughly 76 GWp total. Most of the growth is happening outside of European Union; in 2011 the EU claimed 75% of the PV capacity, whereas in 2016 that share had shrunk to less than 10%. China has turned into the goliath of the PV market,

11

Table 2.1: Characteristics of the chosen PV model

Variable	Value	Unit
P_{MP}	260	W
I_{MP}	8.59	A
V_{MP}	30.3	V
I_{sc}	9.09	A
V_{oc}	37.7	V
η	17.7	%
$NOCT$	319.15	K
A	1.62	m^2

possessing nearly half of the total generation capacity (34 GWp). By 2020, it is expected that the cumulative world PV generation capacity will reach just shy of 100 GWp. Furthermore, it is forecast that PV will go from generating 1% of the total global electricity consumption in 2015, and swell to 30% by 2050 [26].

One main driving force behind the growth of the market has been the continually falling prices of PV modules. In the beginning of 2009 a poly-crystalline silicon PV module cost around 3.40 \$/Wp, and by the end of 2016 the price was under 0.50 \$/Wp. Coupled with that has been the severe drop in the polysilicon price that occurred in 2009. The price started that year being roughly 450 \$/kg and ended 2009 at just above 50 \$/kg, the price continued to slowly fall over the next few years and has now stabilized at just below 15 \$/kg. One other main catalyst for the price reduction has been the increase in efficiency of the PV modules. As of 2016 the average commercial module efficiency (not only poly-crystaline silicon, but for mono-crystalline as well) was approximately 16%, and this number is expected to linearly improve to 20% by 2025, and eventually 30% by 2050 [26].

In addition to PV laying claim to a much larger market share, moving forward carbon pricing is going to assist in forcing to utility companies to turn away from fossil fuel fired power plants to green alternatives. Increases in carbon pricing will have a double impact; it will raise the operating costs of plants that produce emissions and it will reduce the rate at which these plants get dispatched by the utilities [27].

2.1.5   Choice of PV Module

There are innumerous commercial PV modules on the market today, each possessing its own strengths and weaknesses. For this analysis, the Yingli 260-29b was chosen because it is one that Lark Energy traditionally uses. The key performance metrics for this module can be seen in table 2.1 and for further information the data sheet can be found in Appendix A.1.

2.2 Electrochemical Batteries

There are many categories of electrochemical batteries, each with their unique operating principles and inherent advantages. This paper will analyze a few of the more promising battery types that are currently being considered by the industry to be a viable option for grid level electricity storage.

2.2.1 Functional Theory

Lead Acid Batteries

This battery type is by far the most tested and proven on the market today due to the fact that they are less expensive than most other chemistries, reliable and perform well. This battery consists of a lead (Pb) anode (negative electrode) and a lead-oxide (PbO_2) cathode (positive electrode) which are submerged in a hydrogen sulfide (HSO_4) electrolyte. During the discharge process, an external load is applied causing electrons to flow from the anode to the cathode. As it is discharging, the charge and voltages of the electrodes is being reduced, and the electrolyte is diluting and forming a lead acid ($PbSO_4$) solution that coats both electrodes. Alternatively, during the charging phase, the electrons flow from cathode to anode, the charge and voltage of the electrodes increases, the $PbSO_4$ reconstitutes into Pb and PbO_2, and the electrolyte concentrates once more. The typical cell voltage for a lead acid battery is 2.05 V [28].

Lithium Ion Batteries

Lithium Ion (Li-ion) batteries have come a long way in the past several decades, and researchers have been focusing their efforts to push the envelope even further moving forward. The great interest in Li-ion batteries come from its unmatchable combination of high energy density and high power density, which is achievable because of the fact that lithium is the lightest (density of 0.534 g/cm^3 at room temperature) and most reactive metals [29].

The batteries are usually a combination of a metal oxide cathode (e.g. Cobalt oxide) and a carbon-based anode (e.g. graphite), with the electrolyte consisting of lithium salt in an organic solution. During the charging and discharging state the lithium ions flow back and forth between the structures of the metal oxide and graphite. Charging the battery causes lithium ions to separate from the metal oxide and to fill openings the carbon lattice, whereas discharging results in the ions freeing themselves from the carbon and returning to intercalate in the metal oxide layered structure [30]. The nominal voltage of a standard li-ion battery cell is 3.7 V [29].

Liquid Metal Batteries

These batteries are still in their infancy from a commercialization perspective, but one company called Ambri has made great strides and is close to manufacturing their liquid metal batteries which would be capable of grid level energy

storage. Ambri's plan to keep costs to a minimum was to manufacture a battery out of earth abundant materials, using simple manufacturing techniques [31].

The CEO and man behind this new battery chemistry, Donald Sadoway, was so confident that his idea will succeed in the future that he spoke about it during a TED Talk in 2012 in which he revealed several details about the battery's characteristics. The batteries consist of a liquid magnesium negative electrode and liquid antimony positive electrode, and separating the two is the electrolyte layer which is composed of molten salt. In order to produce current, the magnesium expels two electrons and then passes through the electrolyte, becoming Mg_2I (magnesium ion) and finally moving into the positive electrode where it accepts two electrons and forms an alloy Sb-Mg. It is the current passing back and forth through the electrodes that generates enough heat to maintain the metals in their liquid state (operating temperature is roughly 700^0C) [32].

Zinc-Air Hybrid Batteries

Typically, a metal-air battery is non-rechargeable but when a third electrode is added, it allows the batteries chemical processes to be reversed and charged [33]. In this vein, Eos Energy Storage has developed a battery consisting of a zinc anode, an air-breathing cathode, a salt water aqueous electrolyte, and a second cathode made out of a zinc hybrid. The zinc hybrid enables the battery to be replenished with liquid as needed during the recharge phase [34].

Vanadium Redox Flow Batteries

There are many types of flow batteries, however the vanadium redox flow battery (VRFB) is the most studied of the genre having been investigated since 1986 [35]. As is the case with many other battery types, a VRFB consists of two chambers (a positive and a negative electrode), which are seperated by an ion-exchange membrane. Each chamber is filled with electrolytes composed of vanadium in some form; the cathode circulates a VO_2^+/VO^{2+}mixture and the anode holds a V^{2+}/V^{3+}mixture. When the battery is discharging, the VO_2^+reduces to VO^{2+}allowing the positive electrode to give off an oxygen, which passes to the negative electrode causing the oxidation and conversion of V^{2+}into V^{3+}. The typical cell voltage for a vanadium redox flow battery is 1.25 V [36]. There have been investigations into other chemistries and into the replacement of one of the electrolytes, for example substituting in iron or a hydrochloric-sulfuric acid mix, which have shown promising test results but are not yet commercially available [35].

2.2.2   Key Performance Metrics

The key categories that are analyzed when assessing battery value are energy density, number of cycles in the battery's lifetime, length of lifetime, efficiency, and perhaps most importantly, price.

Table 2.2: Performance characteristics for several types of electrochemical battery

Battery	Specific Energy [Wh/kg]	# of cycles	Lifetime [yrs]	Efficiency [%]	Price [$/kWh]
Lead Acid	25-40[28]	2000-4500[39]	5-15[39]	70-90[39]	150[28]
Li-Ion	150-350[29, 39]	1500-7000[38, 39]	5-15[39]	85-95[39]	250[37]
Liq. Metal	20[31]	10000[31]	15[31]	75[31]	-
Zinc-Air	28[34]	5000[37]	15[37]	75[37]	160[37]
VRFB	25-35 [40]	10000[37]	30[37]	70-75[37]	500 [37]
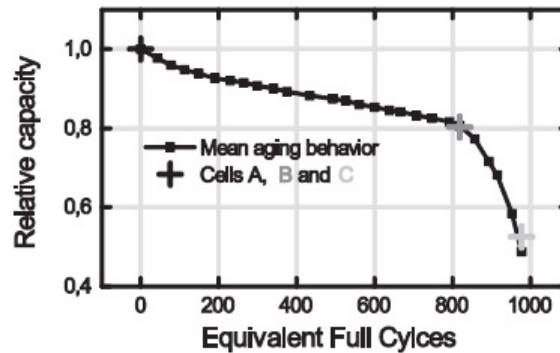
Figure 2.5: Degradation of battery capacity over lifetime [41]

It can be seen by examining table 2.2, that although new technologies such as the Liquid Metal and AHI batteries are starting to enter the market, it is hard to compete with the Li-ion batteries, especially as their price continues to fall.

2.2.3 Battery Degradation and End of Life

One important element of modeling battery performance is the need to consider how a battery degrades over the course of its lifetime, as well as defining how exactly to classify the lifetime of the battery. There is some debate concerning the point at which a battery no longer becomes operationally functional, with some saying that it occurs at as low as 65% or even 50% of initial capacity, however a majority of researchers agree that the End of Life (EOL) for a battery occurs when a battery reaches 80% of its initial capacity [41].

Surveying the data in figure 2.5 leads to the conclusion that although a battery still operates after the 80% capacity threshold, its capacity begins to rapidly reduce and makes the battery much less useful and reliable [41].

For the purposes of this simulation, the assumption was made that batteries would need to be replaced once they degraded to the point of possessing 80% of their initial capacity. Now that the EOL has been chosen, the other simulation

related consideration is determining how to model the continual degradation of the battery.

Wankmüller et al. attempt to quantify the amount of degeneration that a battery experiences during a lifetime of continual charging and discharging; in this particular case, they examined batteries used for energy arbitrage (the concept of buying energy when the price is low, storing it, and then selling it back when the price is high). Below is a formula (equation 2.11) that they developed to quantify the remaining charge (Q_{rem}) in a battery after a given period t has passed [42].

$$Q_{rem}(t) = 1 - \frac{f_{BA} \cdot TE(t)}{\eta} \qquad (2.11)$$

f_{BA}, the battery fade factor, is estimated to be 2.71x10-5. They also tested a model that utilized a different fade factor (3.37x10-5), which was obtained via a linear curve-fitting process. As a result of implementing the degradation into the analysis, a drastic reduction of the battery's Net Present Value (NPV) after 10 years can be seen. After the 10-year mark, a battery with zero degradation is expected to have an NPV of 358 $/kWh, whereas the degraded battery will see its value fall to somewhere within a range of 194-314 $/kWh depending on the degradation model used and assumptions about when end of life will occur [42].

2.2.4 Battery Operational Strategy

There have been many studies performed in recent years attempting to determine how to best dispatch batteries so that both their lifetime and revenue potential can be maximized. In the first study, carried out at Sandia Labs, the researchers sought to determine the maximum potential revenue for a grid connected electricity storage system and did so by comparing two different strategies for revenue generation. The first strategy was simply to use the storage to facilitate electricity arbitrage, and the second strategy being a combination of energy arbitrage and grid frequency regulation services. The study concluded that not only was providing grid frequency regulation far more profitable (approximately 4 times better), but that it was also extremely difficult to implement an accurate algorithm for system electricity prices that would make arbitrage more competitive. It was determined that using energy storage to provide frequency regulation services ultimately could yield 95% of the theoretical maximum revenue of an energy storage technology.

Yet operating a battery storage system in this manner is harmful to the battery's performance in the long run. One potential method to combatting this battery degradation, proposed and tested by van Haaren et al., was to keep the battery's state of charge (SOC) within a range of 40-60% of full charge. This helped to reduce the number of times that a battery would either be discharged too low or get overcharged, and in the long run, enhanced the battery lifetime [43].

Table 2.3: Table showing how the raising the minimum allowable SOC for a battery can affect lifetime and system revenue [45]

SOC_{discon}	SOC_{recon}	Met/Unmet load [%]	Exp. Life [yrs]	Total NPC [$]	LCOE [$/kWh]
0.2	0.3	99.99/0.01	5.2 (-10.3%)	24938	0.81
0.3	0.5	99.96/0.04	5.8 (base case)	24291	0.80
0.4	0.5	99.93/0.07	6.3 (+8.6%)	22408	0.72
0.5	0.6	99.84/0.16	6.8 (+17.2%)	21413	0.69
0.6	0.65	99.75/0.25	7.5 (+29.3%)	20260	0.65

Using this as an operating parameter, Bullich-Massagué et al. have developed two separate operating strategies for responding to grid frequency events based on the SOC level of their BESS. The first strategy seeks to always have the system SOC be 50%, and to only vary due to a lack of PV production or a curtailment period. The other strategy was to apply an equation that has the SOC follow the measured power generated by the PV system, while staying within its preset range [44].

$$SOC^*(t) = 0.4 + \frac{0.6 - 0.4}{P_{plant}} P_{pv-meas}(t) \tag{2.12}$$

The results of the study indicate that following the second strategy allows the battery to stay less stressed on days with high variability in irradiance. Strategy 2 also proved to be superior in its ability to reduce the amount of time that the SOC ventured out of the preferred operating window (an 8% reduction shown during a 43-day test period) [44].

The work of Dufo-Lopez et al. shows that as the minimum allowable SOC is increased, so too is the expected battery lifetime. The table shows how raising the SOC % at which the batteries are disconnected from the load (SOC_{discon}) and reconnected to the load (SOC_{recon}) can affect the percentage of load that is met or unmet, the expected lifetime of the batteries, the total net present cost (NPC) of the system, and the LCOE of the system.

2.2.5 Issues

It must be stated, that none of these battery types are without their faults. They all possess certain character flaws that hinder their performance and usage under certain conditions.

Lead Acid

- Overcharge will result in the release of gas and corrosion of the positive grid, leading to structural weakness and ultimately, failure [28]

- Sulfate accumulates on the negative electrode, leading to failure [28]

- Aged Pb plates result in short-circuit of the cells [28]

17

- Electronically conductive materials can fall to the bottom of the cell and electrical shorting can occur between electrodes[28]

Li-Ion

- An increase in temperature can decrease the number of cycles [29]

- The formation of lithium dendrites can lead to short-circuit failures, fire, or even explosion [29]

- Damage to the cell can cause thermal runaway [29]

- Structural changes yielding reduced integrity may occur in the electrode material during cycling, stemming from continuous expansion and contraction [29]

Liquid Metal

- Need to operate at a very high temperature, around 700 ^{0}C [31]

- Not yet commercially available, still in the last stages of testing and thus unproven in real-world applications [31]

Zinc-Air

- Susceptible to morphological changes of the zinc negative electrode [33]

- Air electrode can fail due to unwanted pollutants [33]

Vanadium Redox Flow

- Low volumetric energy storage capacity [36]

- Vandium is expensive and requires high temperature operations to guarentee its purity, which further drives up costs [35]

2.2.6 Choice of Battery

In order to pick the correct battery for this particular system, the requirements of the application must be considered. The batteries need to provide a minimum electricity generation capacity for up to 30 minutes at a time (see secondary frequency response requirements in section 2.6.2.2). In certain situations, the batteries will also be called upon to charge from the grid to provide regulation in the other direction (meaning they will need to charge with electricity from the grid in order to reduce the grid frequency). Since it was specified by Lark that their planned power plant site has space limitations, it makes the most sense to select a Li-Ion battery for this thesis. Lithium-Ion batteries have the best energy and power density, are commercially proven and although they are not the best in terms of cycle life or price, their performance in those categories
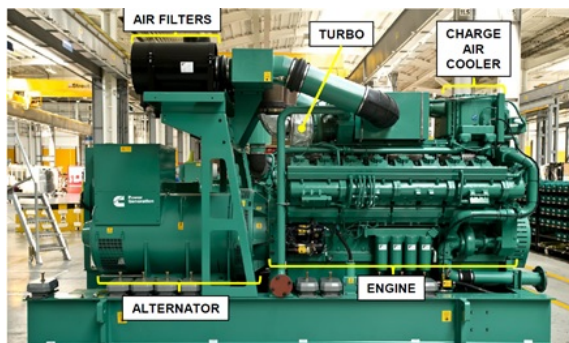
Figure 2.6: Gas generator with component labels [46]

is not so far removed from the other choices. Data sheets for all the lithium-ion battery system utilized by the simulation can be found in Appendix A.2.

2.3 Gas-fired Generators

A gas generator, commonly referred to as a genset, is a piece of electro-mechanical equipment that burns natural gas and converts it into electricity.

2.3.1 Operational Theory

There are two major components to any genset, the engine and the alternator. Of course, there are several ancillary components that help the engine to function properly (such as the charge air cooler, the turbo and air filters), but it is the engine which converts natural gas into mechanical energy which drives the alternator and in-turn generates AC electricity.

Most genset engines are also equipped with an electronic control system (ECS), allowing for remote control and rapid adjustment of the generation level. Additional features of the ECS typically include:

- Automatic digital frequency synchronization and voltage matching

- Isochronous load sharing

- Droop kW and kVar control

- AC bus metering and protection

- 24-VDC battery operation; to ensure that the ECS doesn't rely on external power to function

- Status monitoring of all critical engine and alternator functions [47]

A genset's performance can be judged on mechanical efficiency, electrical efficiency, fuel consumption, or amount of harmful pollutants emitted. An average value electrical efficiency for unit is around 40%, after losses to exhaust heat and radiated heat are accounted for.

Another consideration that needs to be made is partial loading. While operating under 100% load conditions a genset has a specific value for efficiency, fuel consumption and emissions, but when the load is reduced to 75%, or even worse 50%, these values worsen. The overall fuel consumption decreases, but the amount of fuel burned to produce each kW of electricity increases. Similarly for the emissions, the total exhaust being expelled by the engine decreases, but the ppm count of certain harmful gases goes up [48].

2.3.2 Importance to System

In an application such as this where at any given moment the system may be called upon to provide a certain level of electricity to help stabilize the grid, gensets serve as fail-safe to be used if the other options are incapable. If there is a day with low levels of irradiation, the PV panels will not be able to meet their output capacity requirements or even sufficiently fill the batteries, leaving a void that must be filled by the gas generators. The gensets can assist in charging the batteries or directly feeding electricity into the grid, if need be.

2.3.3 Choice of Gas-fired Generator

Lark Energy requested that a Cummins gas-fired generator, either one of the QSK60 or QSV91 models, be used since they had a previous working relationship with the company. These 4-stroke cycle gensets all produce AC electricity at 50 Hz and come in power capacities ranging from 995 kW to 2 MW [48]. Data sheets for all of the genset models considered in the simulation can be found in Appendix A.3.

2.4 Hybrid PV Systems

The focus will now shift to different hybrid energy systems (HES) that have been implemented in the past, including what technologies they utilized, what advantages their hybridization offered and how their respective technological capacities were established and optimized. The two works that were chosen were: "Feasibility study and sensitivity analysis of a stand-alone photovoltaic–diesel–battery hybrid energy system in the north of Algeria" by Rezzouk et al. (section 2.4.1) and "Assessment of decentralized hybrid PV solar-diesel power system for applications in Northern part of Nigeria. Energy for Sustainable Development" by Adaramola et al. (section 2.4.2).

Table 2.4: Table showing how increasing the percentage of PV contribution affects the system costs [49]

PV contribute (%)	Capital ($)	Replacement ($)	O&M ($)	Fuel ($)	NPC ($)	LCOE ($/kWh)
25	271,111	185,551	64,761	122,694	617,489	0.260
50	672,497	147,141	63,197	75,469	885,813	0.374
75	5,597,393	1,750,556	528,468	41,362	6,944,177	2.924
100	13,177,640	4,085,969	1,278,336	0	16,251,960	6.904

2.4.1 Stand-alone PV/Diesel/Battery System

This study examines five different scenarios for generating electricity to cover the demand of a facility in the north of Algeria. Each scenario assumes a different level of PV penetration, ranging from 0% (only diesel generators) to 100% (PV-BESS combo, with no generator back-up). Due to the low cost of diesel (Algeria is among the world's top ten countries for lowest diesel price) and the hefty investment required for PV and battery systems, the stand-alone diesel system was found to be the most cost effective. The system generated a net present cost (NPC) of over $330,000 and had a LCOE of 0.142 $/kWh. Surveying the data in table 2.4, it can be seen that as the % of PV contribution increases, so too does the LCOE and NPC [49].

The authors then provide further considerations, such as avoided emissions and a sensitivity analysis concerning the price of diesel. After weighing the additional information, it is their conclusion that the 25% PV-diesel-battery HES is "economically optimal system."

2.4.2 Decentralized Diesel/PV/Battery Hybrid System

In this paper, the researchers aim to find the optimum combination of four technologies (photovoltaic cells, diesel generators, batteries and power converters) in order to suffice the electricity demands of a region in the north of Nigeria. The area had an average daily irradiance of 6 $kWh/m^2/day$ and at the time of the study the diesel price was taken to be $ 1.1/L. Their simulation compared the results for four different configurations: a generator only system, a generator/battery system, a PV/generator system, and lastly, a PV/generator/battery system. The optimal HES was found to be the fourth configuration, consisting of 175 kW of PV, 260 kW of generators, 694 kWh of battery storage and a 150 kW converter [50]. The financial specifics of the 25-year system outlook are presented table 2.5.

The LCOE for the proposed solution was estimated to be $0.364/kWh, which compares favorably to all the alternatives (stand-alone generator = 0.42 $/kWh, generator/battery = 0.425 $/kWh, PV/generator = 0.387 $/kWh) [50].

Table 2.5: Table enumerating the investment costs for each component utilized in the hybrid system [50]

Component	Capital (1000$)	Replacement (1000$)	O&M(1000$)	Fuel(1000$)	NPC(1000$)
PV	560.0	0.0	30.5	0.0	59.0
Generator 1	33.9	18.0	51.8	1033.7	1123.8
Generator 2	19.3	25.5	72.5	1229.8	1343.3
Converter	36.8	23.6	0.0	0.0	54.4
Other	75.0	0.0	26.1	0.0	101.1
System	725.0	67.1	180.8	2263.5	3213.2

2.5 Frequency Balancing

In this section, the issue of grid frequency balancing is addressed by providing an explanation of the fundamental principle behind this concept, analyzing requirements of frequency response services, and also mentioning the financial implications of this sector of the electricity generation market.

2.5.1 Fundamental Principle

To put it simply, the electrical frequency (also known as power frequency) refers to the rotational speed of the turbines and generators that are generating electricity. As previously stated, too large of fluctuations in the frequency of electricity provided by the grid can be potentially damaging to equipment or result in blackouts, both of which can be costly to a number of parties. The stems from the fact that when rotating at a given speed a turbine (or generator) possesses a given amount of kinetic energy. If the electricity demand increases above the supply, the turbine tries to compensate this by giving away some of its kinetic energy, which in turn reduces the rotational speed of the turbine, thus also reducing its rotational frequency (see equations 2.13 and 2.14) [51].

$$KE = \frac{1}{2}I_{mo}\omega^2 \qquad (2.13)$$

$$f = \frac{\omega}{2\pi} \qquad (2.14)$$

Since the moment of inertia (I_{mo}) of the turbine blades is a fixed value, the only variable that can change is the rotational (angular) speed (ω) [52].

Part of the design of both turbines and generators dictates that they maintain their rotational speed within a certain frequency range. The standard range for such pieces of equipment is ± 0.5 Hz. Once the rotational speed reaches the upper or lower boundary of this range the equipment automatically shuts off to eliminate the risk of damage, and if they are forced to shut down then it put excess stress on the remaining pieces of grid-connected equipment. In many cases the unplanned shutdown of a grid-connected turbine will result in an electrical blackout (aka loss of power) in the system [51].
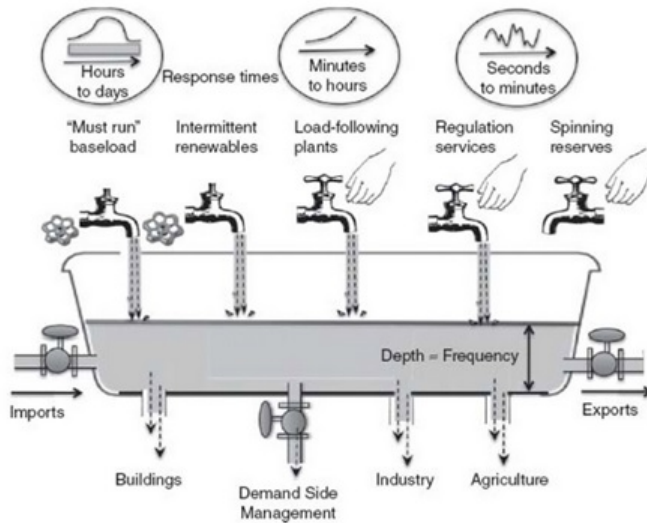
Figure 2.7: Bath tub analogy to represent the contributing factors that affect grid frequency level [2]

Figure 2.7 clearly depicts all of the forces that are at play in the electrical transmission network at any given moment. With so many different electricity production sources feeding into the grid and so many residential and commercial consumers, maintaining a specific frequency is a difficult balance.

Examining the figure (2.7), it can be understood that if the rate of production start to increase above the rate of consumption, the frequency level is going to rise; whereas having more electricity consumption than production will result in the frequency falling to sub-optimal levels. Most of the generation categores displayed in the figure are pretty simple concepts; baseload plants are constantly running at a fixed level to cover the base electricity demand, intermittent renewables are self explanatory, and load-following plants are those which are constantly adjusting their output as the demand level changes. Then there are regulation services, which applies to plants (like the one being considered in this thesis) which are already online and producing but only are required to alter their production, or maintain a certain level of production depending on the circumstance, in the event of a major frequency deviation [53]. Finally there are the spinning reserves, these are generation plants that are constantly on-line but are not under a full load. When there is a transmission outage from other generation resources the spinning reserves increase their load to compensate for the deficit, and they are typically the first to be called upon during an outage [54].

23

2.5.2 Requirements

At a global level, there are two main frequency levels that are utilized, 50 Hz and 60 Hz. For logistical issues, nearly all countries (save a few strange cases, i.e. Japan and North Korea) and their neighbors elect to keep every operating at the same frequency. This ensures both stability and enables easy importation/exportation of electricity between bordering countries. Essentially all of the Americas (North, Central and the northern half of South), plus Saudi Arabia operate at 60 Hz, and the rest of the world operates at 50 Hz [55].

The specific frequency response requirements for this particular case are discussed in greater detail in section 2.6.

2.5.3 Financial Implications

In 2014, the UK's commercial frequency response market was worth a reported $168 million. This figure represented 23% of the ancillary services market and the plants offering this service were paid roughly $69,200 per MW per year. Since the National Grid requires a minimum of 10 MW of capacity to qualify for a tender, each tender holder can expect to earn at least half a million in revenue annually [56].

2.6 UK System

An overview of the potential end customer for the proposed hybrid plant (National Grid) shall be made to provide some greater detail about the scope of application.

2.6.1 System Overview

From the end of February of 2013 to end of February of 2016, the installed off-grid PV capacity went from 1.6 GWp to 9.3 GWp, an increase of nearly 600%. Due to this increasing PV capacity, National Grid has seen a reduction in their summer demand. In 2014 and 2015 the peak summer time demand was 38.5 GW and 37.5 GW, respectively, and for 2016 they had projected it to be 35.7 GW. Figure 2.9 shows the monthly energy demand for the UK over a 10-year period. It can be seen that the blue line depicts a downward trend in the demand, which is mainly being caused by the embedded PV generation along with efficiency increases in both buildings and technologies [57].

2.6.2 U.K. Markets

2.6.2.1 Electricity Market

The electricity market in the United Kingdom consists of many players, from regulatory authorities (Office of Gas and Electricity Markets or OFGEM) to transmission operators (NGET), suppliers, generators (Lark and their customers),
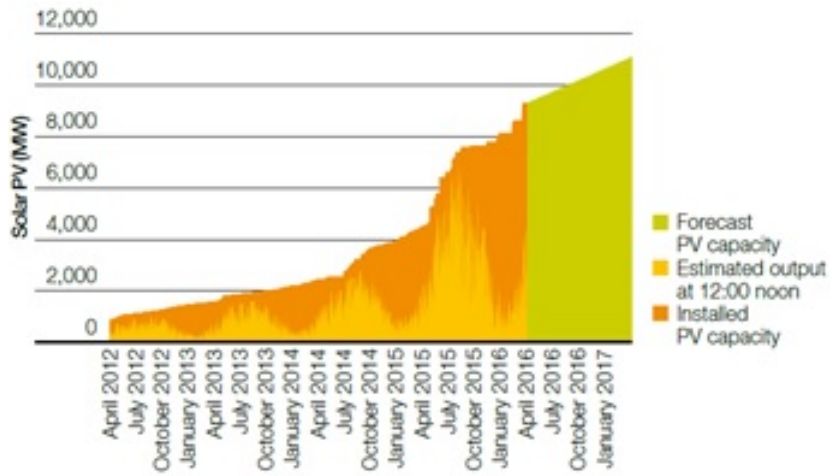
Figure 2.8: Depiction of the recent growth in the installed solar PV capacity in the UK [57]
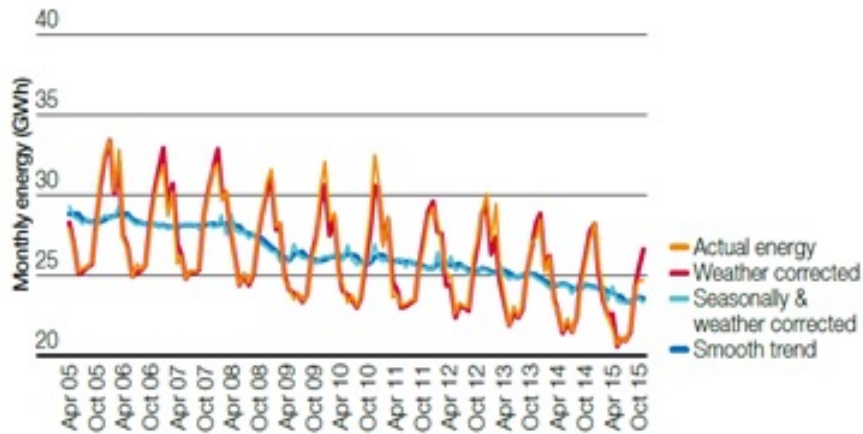
Figure 2.9: Monthly energy demand in the UK over the past ten years [57]

traders and finally, customers. OFGEM main function is to protect the current and future interest of the end consumers and seek to do this by promoting secure and sustainable options, as well as by fostering competition between suppliers and generators [58].

The real-time and historical prices are made available to the customers through the Nord Pool Market platform. Through this platform all interested parties can gather data regarding market trends and tendencies so that they may produce or consume in the most efficient or economical manner. Going beyond that, thanks to the Day-Ahead Price Market (UK N2EX) existing in the UK, these same parties can plan their optimal operation strategy for the coming day [59]. This allows electricity generators to best allocate their resources and enables customers to avoid consuming during peak price hours.

For the analysis associated with this report, the evaluation of the ideal power plant was made based on the Nord Pool electricity price data from 2016.

2.6.2.2   Frequency Response Market

National Grid, like the rest of Europe, transmits electricity at 50Hz. They maintain a tight tolerance on their frequency control; only +/- 0.2Hz is considered within the acceptable operating range. Anything outside of this range must be responded to within 10 seconds [60].

As part of their operating procedure, National Grid defines a few different varieties of frequency response. Those being: Primary Response, Secondary Response and High Frequency Response. Primary Response is defined as the "provision of additional active power (or a decrease in demand) within 10 seconds after an event and can be sustained for a further 20 seconds". Secondary Response does not have to react as quickly (30 seconds after an event) but must be sustained for a much longer period (30 minutes). High Frequency Response is a bit different, because it results from there being too much electricity generation flowing into the grid, and thus the requirement is a reduction of generation within 10 seconds and this reduction must be maintained for an indefinite period of time [60].

Demand Response is a service that National Grid has procured since the year 2007. They have contracted in the range of 200-700 MW per year of Primary Response and in the range of 700-1400 MW per year of Secondary Response. Returns for these response plants ranged from 22,500-30,000 $/MW for Primary Response and as much as 45,000-60,000 $/MW for Secondary Response [61].

Data provided by National Grid for the year 2014 displays how many times the grid frequency was outside of the operational limits (see table 2.6). The data was only given for the first week of each month, and from it daily, weekly and monthly averages were tabulated.

It can be seen that the summer months (June-September) experience less frequency response events on average. Overall, the yearly average dictates that there is just more than one event requiring frequency response every day, on average. The next graph shows at what hours of the day these events typically occur.

Table 2.6: Table enumerating the high, low and total frequency events that occured in the UK during 2014

Month	High	Low	Total
Jan	8	5	13
Feb	10	6	16
Mar	8	1	9
Apr	11	9	20
May	7	4	11
Jun	2	1	3
Jul	0	4	4
Aug	0	0	0
Sep	2	1	3
Oct	7	2	9
Nov	2	1	3
Dec	6	3	9
Total	63	37	100
Avg. day	0.75	0.44	1.19
Avg. week	5.25	3.08	8.33
Avg. month	22.75	13.36	36.11
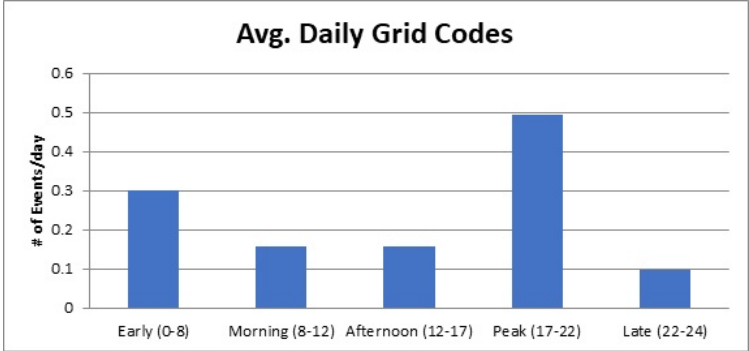
Figure 2.10: Graph illustrating the occurences of high and low frequency events during different periods of the day

With 1.19 events occurring every day and 0.49 events happening during the peak hours, it can be shown that, on average, 41% of all frequency response events take place between the hours of 17:00 and 22:00 (20.8% of the day).

2.6.2.3 Capacity Market

As of 2016, 26% of the EU's power is produced from renewable sources, with 10% of the total electricity generated from intermittent sources (capacity mechanisms report, European Commission 2016). As renewable energies come to represent a larger segment of a countries' generating capacity, older fossil fuel burning plants shut down and potentially leave a large gap in the baseload capacity. With conventional fossil fuel plants now or in the near future closing their doors, many concerns were raised that a void would be created and leave countries unable to provide a stable electricity supply. To prevent this from occurring many countries are looking into implementing a Capacity Market in the electricity generation sector, a tool aimed to ensure that countries have a secured generation capacity for the future. In this regard, the UK is slightly ahead of the curve since they put their Capacity Market into effect starting in the fall of 2014 [4].

The UK capacity market functions by holding an auction once a year where electricity producers provide bids representing the amount (in MW), the rate (in $/MW) at which they can generate and the amount of time (in years) that they plan to operate. One caveat is that they are not promising their production for the following year, but rather a period that starts four years in the future. The UK must accept bids until they have satisfied the required level of generation that they have forecasted for the future. Once all the bids have been placed and the generation needs have been met, contracts are established and each plant receives a tendered amount equal to the highest bid price that was accepted [62]. To put it another way, a theoretical situation could exist in which a country needs a total of 150 MW and they could potentially receive the following bids:

- A 50 MW solar PV plant offering its capacity at 50 $/MW

- A 50 MW wind farm offering its capacity at 30 $/MW

- A 50 MW hydro power plant offering its capacity at 25 $/MW

- A 50 MW natural gas fired CCT plant offering its capacity at 35 $/MW

In this scenario, the country would choose to accept the bid offers from the wind farm, hydro plant and natural gas plant, and it would have to pay each one of them 35 $/MW. Thus, both the wind farm and hydro power plant would receive an additional 5 and 10 $/MW, respectively, over their required operating costs.

Down the road, if one of the plants realizes that it will be unable to meet its contracted obligation, due to maintenance or unforeseen issue, another Supplementary Auction is held so that other plants can bid to cover this newly available production requirement. The original plant is then obliged to pay for the cost of the winning bid, however, if this new bid ends up being lower

than their original contracted price, the plant will still make some money while having provided no capacity [62].

2.7   Design Location

The chosen design location coincides with one where Lark Energy currently maintains a solar farm in the UK. At the request of the company, the exact location information is not published in this report, yet the atmospheric and geographic conditions have all been taken account in the calculations.

Chapter 3

Methodology

This chapter provides an explanation as to how the different hybrid plant models were developed and how their yearly performance was simulated. These simulations were carried out with the help of a combination of different pieces of dynamic modelling software, which allowed for the calculation of a myriad of plant technical characteristics, energy production figures and economic performance indicators.

3.1 Software: DYESOPT

The main tool utilized during the commission of this work was DYESOPT. DYESOPT stands for Dynamic Energy System Optimizer and it is a MATLAB based tool that was developed by researchers at the Royal Institute of Technology in Stockholm, Sweden. Figure 3.1 is a flow chart depicting the inputs, outputs and processes that are central to DYESOPT's functionality.

    As depicted in figure 3.1, for it to properly complete its calculations DYESOPT needs to be provided with the following:
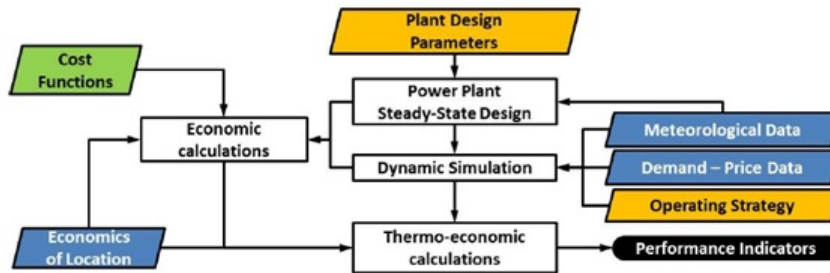
Figure 3.1: Flowchart depicting the main inputs, operations and outputs of the DYESOPT tool and the order in which the processes occur [63]

- technologies to be used (i.e. Solar PV, CSP or gas generators)

- location (which determines meteorological data and price data)

- preferred operational strategy (baseload or peak-hour coverage)

- economic parameters (such as the countries sales tax rate or capital interest rate)

- financing structure (e.g. single owner)

With all of this information DYESOPT can then run a simulation which will calculate the production of the plant for every hour of the year (or less, if specified), the losses incurred by the equipment or operating strategy, plus the capacity factor of each piece of technology utilized. After tabulating the results for one year's worth of operation, DYESOPT then takes this data and extrapolates it – accounting for degradation – to represent the entire production lifetime of the plant. With this, the yearly revenue and operating costs can be established and the determination can be made as to whether or not the plant will be financially viable over the course of its projected lifetime. In this sense, viability is achieved when a plant manages to, at the very least, earn enough income (revenue minus operating costs) to pay back the initial investment plus any interest that had been accrued. Further discussion about financial measurements will be made in section 3.7.

DYESOPT is not fully MATLAB based, in furtherance of carrying out the dynamic calculations required by time dependent dispatch strategies and technological availability it relies upon an additional piece of software called TRNSYS.

3.2   Software: TRNSYS

TRNSYS is described by its creators as "an extremely flexible graphically based software environment used to simulate the behavior of transient systems," more specifically, electrical energy systems [64]. TRNSYS is comprised of two essential parts, the engine/solver and the vast component library. When a simulation is run the engine reads the input file, solves the system of components in an iterative process which continues until a suitable value has been achieved, and then plots out the results.

3.3   PV Model

The photovoltaic system design process in DYESOPT starts on the user end, because before starting any simulation the user must choose from a pre-provided list of PV modules and AC/DC inverters. They must also decide upon a location (for instance, Ouarzazate, Morocco or Sevilla, Spain) and establish their desired total AC output of the system. Upon initiation of the simulation, DYESOPT inherits all of the performance specifications from the PV module (i.e.

rated output power, open circuit voltage, nominal operating cell temperature, etc.) and inverter (max input power, max input voltage, etc.), as well as the meteorological data from the specified location (i.e. daily ambient temperature values, beam and diffuse irradiance levels, etc.). All of this data then generates the boundary conditions for the sizing of the PV system.

As described in the previously referenced work by Larchet, the methodology for sizing the system was based upon research performed by Sulaiman et al., 2011 [65]. Firstly, the predicted max voltage of one module is calculated based on changes to the cell temperature throughout the year, as detailed in the works of Mattei et al., 2006 and Almaktar et al [66, 67]. These voltage values are then used to determine the maximum number of modules that can be connected in series (what is known as a "string") and subsequently connected to an inverter without the inverter's voltage limit. The next step is to establish the maximum number of strings that can be connected to each inverter. This is accomplished by comparing the maximum current that an inverter can handle with the maximum current output of one module. Finally, all of the modules connected both in series and in parallel to one inverter make up one array. The number of arrays required depends upon desired AC output of the farm as a whole and the rated output power of each one of the inverters.

Now that the system has been properly sized, DYESOPT evaluates how much radiation the modules are being exposed to on an hourly basis, for the entire year. To accomplish this a calculation of the sun's precise position in the sky is carried out based on solar geometry. Pairing this with the position and tilt of the modules allows for the percentage of total radiation (beam and diffuse) being absorbed to be approximated. The model is capable of estimating the irradiance levels for fixed-tilt systems as well as for systems with single and double axis tracking. In the case of this work, the data provided by Lark energy was for a 20° fixed-tilt system which faced south. According to Lark, 20° was the optimal for the system given the row spacing constraints of the location, the yield and the mounting structures subcontractor and a fixed-tilt system was chosen due to the fact that the increase in production yielded with a tracking system would not justify the increase in investment cost.

The total irradiance levels on the module surface can be directly translated into the amount of DC power being produced by the solar farm over the course of the entire year. DYESOPT then provides the total AC power yielded, taking into account the inverter conversion efficiency and keeping track of any energy that was curtailed throughout the year due to it being in excess of the limits of the inverter. It can be up to the user to recognize when the plant is suffering to high of inverter losses and to elect a higher rated inverter.

Some additional energy losses that are tracked by DYESOPT include: losses due to self-shading of adjacent solar module rows, losses in the solar farm cables during transmission, losses.

3.4 Battery Model

The sizing of the battery system is carried out by DYESOPT much in the same way as the PV system. Initially, the user needs to select the desired capacity of battery storage and is given the choice of several different battery chemistries (i.e. lead acid and lithium ion). The desired type of connection between battery and power source can also be made, whether it be single stage DC single inverter, double stage DC single inverter or simply an AC connection.

Based on the planned power source, the simulation establishes the maximum possible power, voltage and current that are going to be fed into the batteries over the course of the year, thus giving a boundary condition for the system size. Similar to the PV sizing, the battery system scheme is mostly dictated by the constraints of the chosen inverter. The specific design procedure is carried out by using a simplified mathematical model, which is described fully in the work of Shepard [68]. Typically, the total system capacity is oversized, with regards to the user specified capacity, to account for the fact that many batteries have depth-of-discharge (DOD) limitations. If it is specified by the manufacturers that a certain battery type shouldn't be discharged below a 20% state of charge level, then DYESOPT will oversize the total capacity by 25%. The previously referenced paper by Larchet delves further into the model validation that was performed.

As discussed earlier in section 2.2.3, battery degradation and end of life characteristics need to be strongly considered when running the analysis. To that end, the simulation tracks the number of battery cycles and indicates the years in which the batteries require replacement. From the research that was performed, no standard definition of a full battery discharge cycle could be found, thus a definition was created for DYESOPT. Any time that a battery discharges fully until it reaches its DOD limit, the simulation counts this as a single cycle, and any other time that the battery discharges partially (either the discharge is non-continuous or doesn't fully reach the DOD threshold) it is recorded as a half cycle [69]. One addition that was made in the course of this thesis was to give the user the ability to control the minimum and maximum SOC of the battery so that the causal influence of life prolongation strategies mentioned in other research could be tracked.

One of the last calculations made by the model is the quantification of the battery utilization factor (UF) and the formula used can be seen below.

$$SOC_{diff} : \begin{cases} SOC(i) > SOC(i-1) & SOC_{chrg} \\ SOC(i) < SOC(i-1) & SOC_{dis} \end{cases} \tag{3.1}$$

$$SOC_{chrg} = \sum_{i=1}^{N}(SOC(i) - SOC(i-1)) \tag{3.2}$$

$$SOC_{dis} = \sum_{i=1}^{N}(SOC(i-1) - SOC(i)) \tag{3.3}$$

$$UF = \frac{SOC_{dis}}{SOC_{chrg}} \qquad (3.4)$$

The different in timestep between one timestep (i) and the next determines if the battery is charging or discharging. Then the total percentage of SOC gained and lost during charging and discharging, respectively, is summed for all of the timesteps over the course of one day (N). Finally, the utilization factor is determined by dividing the total energy discharged from the battery by the total energy charged into the battery. The ideal utilization factor of 100% is obtained when amount of energy charged and discharged is the equal for the day.

3.5 Generator Model

The model to simulate the performance of the natural gas generator functions in a similar way to the others, however it is a great deal simpler. Due to the fact that generators are not reliant on external factors such as the environment to function, nor do they require a AC/DC inverter in this model, the design process is a lot less cumbersome. Once the user defines the generator model that will be utilized and the total desired installed capacity, DYESOPT can specify the number of generators required and the total amount of fuel they will consume for every load percentage. The main time that load percentages other than 100% are necessary for the simulation are during the generator's startup/ramp-up sequence.

The model also tracks the total number of operating hours for the generators which will dictate when it is time for them to be replaced.

Standalone Generator Plant Model

Pursuant to offering as many simulation alternatives as possible to help contextualize the results, a model was also developed in which the generators would attempt to provide the FFR services as well. This variation simply couldn't be solved for during the optimization of the combined model due to the fact that it required a different dispatch strategy in order to meet the FFR market requirements. Since primary response (within 10 seconds) and secondary response (within 30 seconds) have response times that are shorter than the length of time necessary for the generators to turn on and come fully online, the conditions suggested that they need to stay running continuously.

The operational strategy for the generators is mainly determined by the frequency value and electricity price and can be seen in figure 3.2.

As depicted in figure 3.2, the generator output is varied between three levels. 30% load is the lowest possible value at which the generator can be run without doing damage to the equipment. 50% load allows for the fuel savings compared to 100% load but still ensure that the generator can be ramped up within 10 seconds in order to meet provide primary response [48]. In addition to running
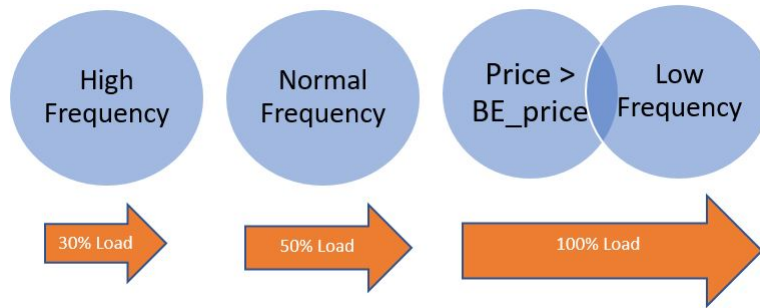
Figure 3.2: This chart displays the conditions which governed the operating load levels of the gas generators

at 100% during times of low frequency, the generator is also run at this level in times when the electricity price is higher than the operating cost of the generator.

This generator only configuration has a few downsides that will be discussed further in the results section.

3.6 Combined Models

3.6.1 BESS-Gen Model

This configuration (see Figure 3.3a) allows for the plant to provide both types of dynamic frequency response while not requiring the generators to be constantly running since the battery can provide energy during the generator startup phase. The generators are present in this configuration solely for the purpose of providing secondary frequency response services, once they ramp up to full-power they run continuously for 30 minutes and then shut off. However, they are not connected to the batteries with the intent of using them to charge the batteries. Instead, the batteries charge from the grid when the electricity price is at its daily minimum or during high frequency events (where the electricity consumed by the batteries is free because the plant is helping to provide a regulatory service).

The dispatch strategy developed for this hybrid plant is one of the central items that was created during the investigation and development of these thesis results. Before the dispatch strategy can be enacted it relies upon some data concerning the market conditions. Thus, after DYESOPT has performed the sizing of the batteries and generators, it carries out an assessment of the electricity market prices for each day of the year and assigns priority charging and discharging hour. The simulation then runs back through and ensure that no priority hour is overlapping with an hour in which the plant is going to be providing a conflicting frequency response service (no discharging of the batteries when the frequency is high or vice versa).

Figure 3.3: Layout of each power plant configuration

(a) Depiction of the BESS-Gen plant config.   (b) Depiction of the PV-BESS-Gen plant config.
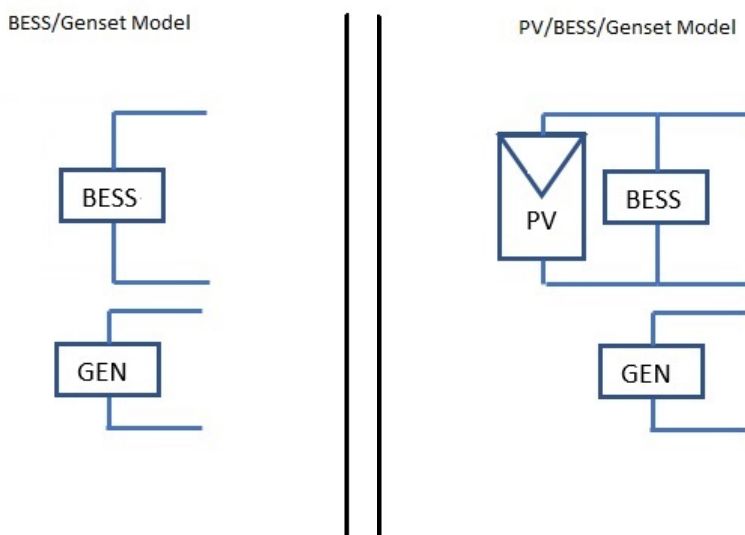
The dispatch strategy is then carried out in the TRNSYS portion of the simulation, so that it can track the dynamic changes in the batteries' SOC, along with how many times the batteries were unable to provide frequency response services. In figure 3.4, a flow chart overview of the dispatch strategy can be seen. After some consideration, it was decided to have the plant offer frequency response 24 hours a day but the flow chart in Appendix C.1 depicts a strategy that accounts for periods before and after the tendered frequency response window.

It can be seen that other than studying the grid frequency and the electricity price, the other major consideration that is made by the dispatch strategy is the SOC of the batteries. In some situations, the battery SOC is either at a minimum or maximum and the market conditions do not encourage charging or discharging, so when this occurs a "no action" command is given and the plant simply stands idle until market conditions change. Based on related literature regarding energy arbitrage through battery storage, it was decided to allow the simulation to investigate the effects of raising the minimum SOC above that of the battery's DOD. If they are providing frequency response services the batteries are allowed to reach their DOD level, otherwise they wouldn't be able to discharge below a pre-set percentage. Later on, the optimization would determine what the best minimum SOC for the batteries would be, in terms of economic performance and maximizing operational life.

Once the dynamic portion of the simulation has completed its iterative process, the model then moves on to tabulate the totals for the first year's op-

erational production, usage and consumption. These values are fed into the thermo-economic calculation script, specifics of which will be addressed in section 3.7.

3.6.2 PV-BESS-Gen Model

The addition of photovoltaic modules to this configuration (see figure 3.3b) adds an extra layer of complexity to the simulation and the dispatch strategy, but the general structure stays the same. The batteries are still looking to charge and discharge at the cheapest and most expensive hours, respectively. The generators are still in place to provide the long-term reliability needed for secondary frequency response.

Before DYESOPT can enter into the dynamic portion of the simulation it is necessary for it to examine how the two chosen technologies (PV and batteries) interlink. Depending upon the specified capacities of the two and the chosen inverter type, it could be that there is going to be curtailment of the PV based upon the maximum charging rate of the BESS relative to the maximum output of the PV or based upon the maximum power rating of the inverter.

The main benefit that this configuration can provide is that the with the PV in place the batteries can use the solar production to charge and avoid paying for electricity coming from the grid. If the batteries are sitting idle at full charge capacity, any PV production can be directly sold to the electricity market. Figure 3.5 is a flowchart that provides a better visualization of how the daily dispatch strategy is carried out.

Examining the flowchart (figure 3.5), it can be noticed that another benefit of having the PV available is that it gives a second method to respond to low frequency events, and acts a contingency in the event that the battery SOC is too low to issue a frequency response. The strategy tries to ensure that as little of the PV production will be curtailed as possible, however, during high frequency events the PV must be curtailed in order to comply with requirements of the FFR tender.

3.7 Financial Performance Metrics

Some concepts must be presented so that it can be understood what the model is looking to achieve.

Net Present Value (NPV)

The Net Present Value (NPV) of a power plant is the representation of the overall value of the project with respect to the current point in time, the year and size of the initial investment, along with the inflation in the value of currency [70]. When estimating the financial future of a project, it is commonplace to set the NPV of the final year of operation equal to zero. In essence, this assumes that the plant will make enough revenue (plus an acceptable level of profit) so that it has paid off the initial investment just before it gets decommissioned.
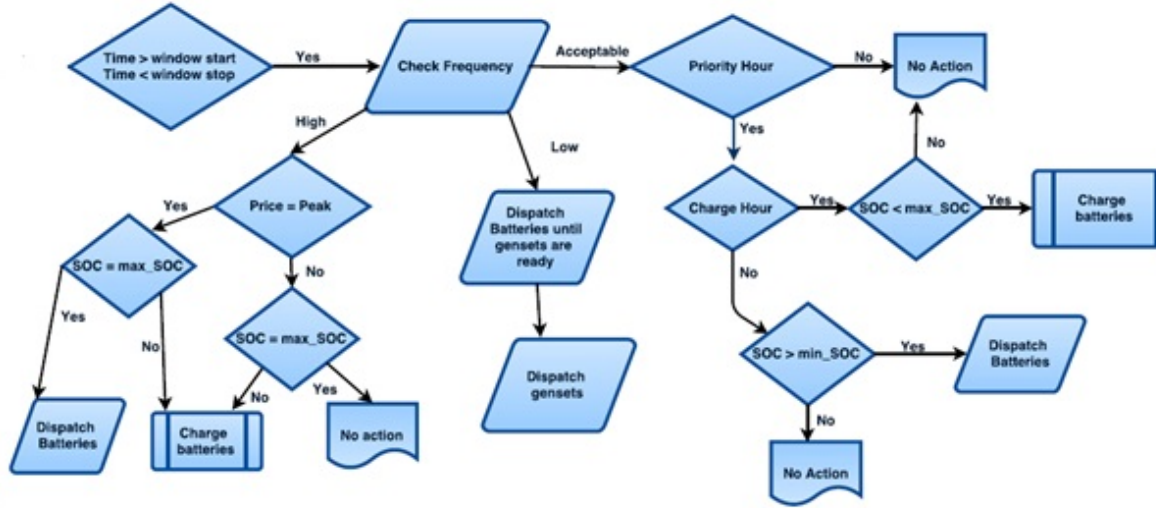
Figure 3.4: Flowchart which shows the decision making process implemented by the BESS-Gen model pursuant to carrying out the dispatch strategy
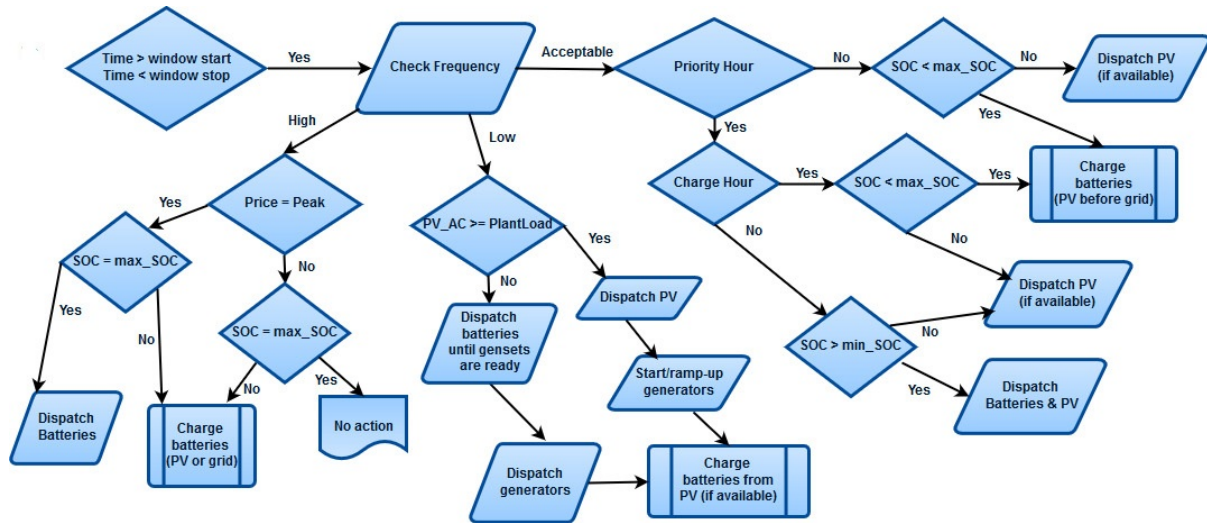
Figure 3.5: Flowchart illustrating the decision making process utilized by the PV-BESS-Gen model to enact its dispatch strategy

$$\sum_{t=1}^{T_{op}} \left(\frac{C_t}{(1+r)^t} \right) - C_0 \qquad (3.5)$$

In equation 3.5, t is the number of years, T_{op} is the final operating year of the plant, C_t is the net cash flow for a given year, r is the discount rate, and C_0 is the project's initial investment (CAPEX) [70].

Internal Rate of Return (IRR)

To understand the Internal Rate of Return (IRR) a discussion of discount rates must first be made. A discount rate is the interest rate of a particular investment as it pertains to future cash flows which are "discounted" by expressing them in present value [71]. This idea is fed by the fact that over time money loses its value; money can lose its value due to inflation or value can be lost in a sense that money not invested would be allowed to earn interest in a bank.

With that in mind, the IRR is simply a very specific discount rate value. It is the value at which the NPV of a project would be equal to zero [72].

Weighted Average Cost of Capital (WACC)

The Weighted Average Cost of Capital (WACC) is a measure of mean interest level for any project a company has on its financial books. This average accounts for projects that were both financed using equity (a company uses its current assets as collateral) and those financed via debt (a company takes out a loan to borrows money).

From a profitability standpoint, comparing the WACC and IRR offers a clear indicator of potential success. If the estimated IRR is higher than the WACC then the project is going to be profitable, whereas having an IRR lower the WACC means that the project shouldn't be pursued. If the two values are equal to one another, the plant is going to break even [73].

Levelized Cost of Electricity (LCOE)

In many techno-economic analyses the Levelized Cost of Electricity (LCOE) is a very useful gauge of the competitiveness of a given plant because it allows for other a comparison of the cost per unit of energy for said plant, irrespective of technology used [74]. However, for this particular application the LCOE doesn't tell the whole story, since a percentage of the revenue of the plant is coming from external sources (FFR and CM payments) which do not directly translate to the electricity production. For this reason, The LCOE was not given any weight in the decision-making process for the design of the plant.

3.7.1 Chosen Parameter Values

The financial parameters decided upon for the here under analysis are as follows:

Table 3.1: Table displaying the different economic parameters that were used as inputs for the simulation (* indicates values that were specified by Lark Energy)

Parameter	Value
Real Debt Interest Rate	5% *
WACC	12% [75]
Sales Tax Rate	5% [76]
Cost of Equity	10% *
Cost of Debt	8% *
Share of Debt	70% *
Rate of Inflation	3% [77]
Plant Lifetime	25yrs *

It was also decided to find the configuration that has a final NPV equal to zero and to set the IRR equal to the WACC.

3.7.2 CAPEX and OPEX Formulas

PV

$$CAPEX_{PV} = C_{direct,PV} + C_{indirect,PV} \qquad (3.6)$$

$$C_{direct,PV} = C_{PV} + C_{Inv} + C_{Conv} + C_{BOS} + C_{tracking} + C_{cont} \qquad (3.7)$$

$$C_{indirect,PV} = C_{E\&D} + C_{Land} + C_{TAX} \qquad (3.8)$$

For the PV capital investment, costs fall into two categories; direct and indirect costs. The direct components are comprised of the PV modules (C_{PV}), the inverters (C_{Inv}), the DC-DC converters (C_{Conv}), the equipment needed to balance the system (C_{BOS}), the cost of the tracking system ($C_{Tracking}$), and some additional contingency costs (C_{cont}). The indirect costs entail the engineering and design costs ($C_{E\&D}$), the cost of land for the farm (C_{Land}) and tax (C_{TAX}). Equations 3.6, 3.7 and 3.8 represent the PV CAPEX equations.

$$OPEX_{PV} = C_{Labor,PV} + C_{Insurance,PV} \qquad (3.9)$$

The OPEX costs consist of the wages of the employees who maintain the plant (C_{Labor}) and the insurance for said workers ($C_{Insurance}$).

BESS

$$CAPEX_{BESS} = C_{direct,BESS} + C_{indirect,BESS} \qquad (3.10)$$

$$C_{direct,BESS} = C_{bat} + C_{PCS} + C_{BOP} + C_{instal} \qquad (3.11)$$

$$C_{indirect,BESS} = C_{E\&C} + C_{soft} + C_{TAX} \qquad (3.12)$$

The cost analysis for the BESS was derived from research performed by EPRI, 2013 [83]. Just like with PV, the battery CAPEX costs are comprised of both direct and indirect segments. Examining the direct CAPEX costs, they are comprised of the battery packs (C_{bat}), the power conditioning system (PCS) (C_{PCS}), the balance of plant (C_{BOP}) and cost of installing the system (C_{instal}). As suggested by the EPRI research, balance of plant costs are assumed to be the civil works costs only [83, 84]. Depending on whether or not the BESS is coupled on the DC side the cost of the PCS can be assumed to be integrated with the PV PCS [83]. The indirect costs encompass the engineering and construction costs ($C_{E\&C}$), the soft costs (C_{soft}) which entail project contingency costs and the tax costs (C_{TAX}).

$$OPEX_{PV} = C_{Fixed} + C_{Variable} + C_{Replacement} \qquad (3.13)$$

The OPEX costs for the BESS is made up of three categories: the fixed costs (C_{Fixed}), the variable costs ($C_{Variable}$), and the replacement costs ($C_{Replacement}$). C_{Fixed} represents the yearly cost of standard operations and the necessary maintenance the PCS. Whereas $C_{Variable}$ symbolizes the costs that come from the discharge of the system, which are mostly made up of electrical efficiency losses and power lost due to self-discharge [83]. The final term, $C_{Replacement}$, is the cost incurred by replacing the batteries once that reached lifetime cycle limit.

Generators

$$CAPEX_{gen} = C_{direct,gen} + C_{indirect,gen} \qquad (3.14)$$

$$C_{direct,gen} = C_{genset} + C_{BOP} + C_{install} \qquad (3.15)$$

$$C_{indirect,gen} = C_{E\&C} + C_{cont} + C_{TAX} \qquad (3.16)$$

As was the case with PV and BESS, the generator CAPEX costs contain both direct and indirect portions. Examining the direct CAPEX costs, they are comprised of the natural gas generators (C_{genset}), the remote controller and components used to balance the genset production (C_{BOP}) and cost of installing the system ($C_{install}$). The indirect costs encompass the engineering and construction costs ($C_{E\&C}$), the contingency costs (C_{cont}), and the tax costs (C_{TAX}) [85].

$$OPEX_{PV} = C_{Fixed} + C_{Variable} + C_{Replacement} \qquad (3.17)$$

The OPEX costs for the generators system has the same rundown as for the battery system. The components include the yearly fixed operating and maintenance costs ($C_{Fixed,gen}$), the variable costs ($C_{Var,gen}$) consisting of the cost of the natural gas consumed and efficiency losses due to operational strategy,
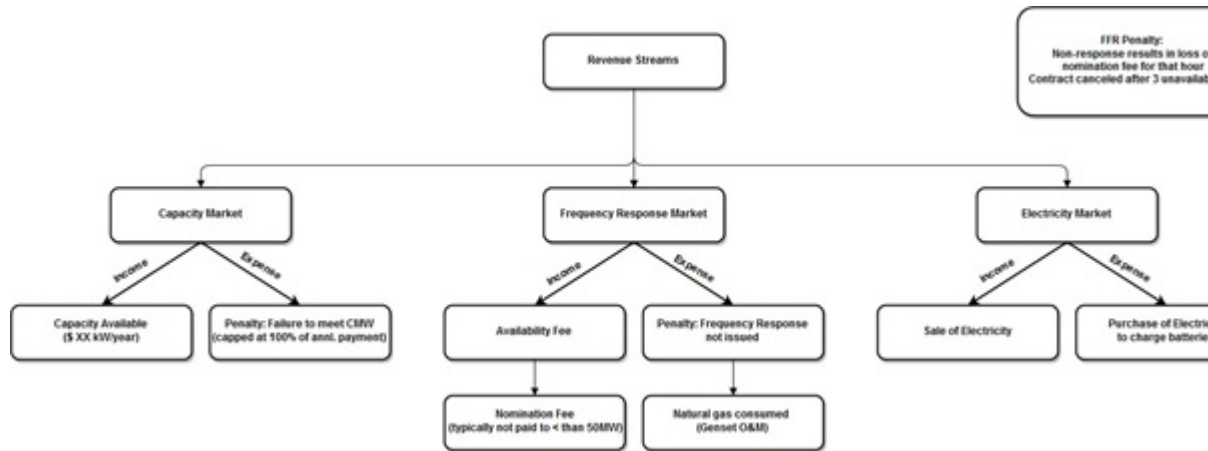
Figure 3.6: Figure portraying the three areas in which the power plant stands to earn revenue

and finally the costs of replacing the generators ($C_{Replace,gen}$) once their lifetime hours of operation limit has been surpassed.

3.7.3 Plant Revenue Streams

Reviewing the chart (figure 3.6) with the knowledge that the capacity market has a pre-established price and that the model uses historical price data for the electricity market, it can be seen that these two values are fixed and thus the only ones that are malleable are the availability and nomination fees of the FFR services.

The availability fee ($/hr) is one which is paid to the FFR provider for each hour of their tendered contract. The nomination fee ($/hr) is awarded to the plant when they actuallly provide services related to a frequency event, so in theory it can be paid to the FFR provider for all or a fraction of the hours in their tendered contract. However, it was stated by National Grid that "Historically, for all tenders that have been accepted, all of the available windows have been nominated" [3]. In a review of all the accepted tender offers for the year 2016 (all made available on the website of UKET, it was discovered that no plant offering less than 50 MW of FFR capacity was given the nomination fee, only the availability. Taking this small contradiction into account, it was decided that in the simulation the nomination fee would be offered to the plant, and that its value would be 50% of the value of the availability fee.

The review of accepted tenders also revealed some useful data concerning the competition. In 2016, many tenders have been awarded to 20MW plants and their nomination fees all fell within a range of 260-450 $/hr (see Appendix B.3). This helped to provide a benchmark as well as a boundary condition for the simulation. To prove that the proposed plant could compete with current

market condition, it needed to be able to operate for a tender fee of equal to or less than its competition.

3.7.4 Revenue Calculation

$$Rev = E_{tot,yield} \cdot E_{price} + CM_{price} \cdot Cap_{plant} + FFR_{fee} \cdot (h + 0.5 \cdot h - 2 \cdot P) \quad (3.18)$$

In which $E_{tot,yield}$ is the total electricity yield (on an hourly basis) from the plant for year one, E_{price} is the electricity price for each hour of the year, the CM_{price} is the Capacity Market auction clearing price in ($/kW/yr), Cap_{plant} is the installed plant capacity in kW, FFR_{fee} is the tendered price for providing frequency response services, h is the number of hours that the services are offered (availability fee), the $0.5 \cdot h$ term represents the nomination fee, and P is the number of non-response penalties that were incurred throughout the year (which is multiplied by a factor of two so that it nulifies the fee payment and assesses a penalty).

With the aim of finding the NPV at year 25 equal to zero, the required yearly revenue must be calculated. Once the revenue is known, equation (3.18) can be rearranged as follows:

$$FFR_{fee} = \frac{Rev - (E_{tot,yield} \cdot E_{price} + CM_{price} \cdot Cap_{plant})}{(h + 0.5 \cdot h - 2 \cdot P)} \quad (3.19)$$

3.8 Multi-variable Optimization

One of the additional functions which DYESOPT possesses is the ability to perform a multi-objective optimization. The optimization seeks to find the best combination of input variables that yield a satisfactory compromise between two variables which typically have conflicting design objectives. This trade-off of the two objectives will produce a curve which is referred to a pareto curve (see figure 3.7) [86].

The simulation uses an evolutionary algorithm which implements a population based approach. In total, the optimization process has four main steps: selection, cross-over, mutation and elite preservation. The entire optimization simulation concludes once either the user-specified requirements have been satisfied or the simulation reaches the maximum number of iterations that was selected. In the early iterations, the optimization generates an initial population, that is constructed based on the work of Leyland, from which some of the more desired points are singled out and are labeled "parents" [87]. These parents are used a reference points from which a new population of "children" can be derived, this is the cross-over step. The children are created by slightly altering some of the characteristics of the parent solutions from which they were formed, also known as the mutation step [86, 87]. Once it is established that the children offer a more ideal solution than the parents, the parents are removed from the population. As it moves forward, the simulation enacts the elite preservation
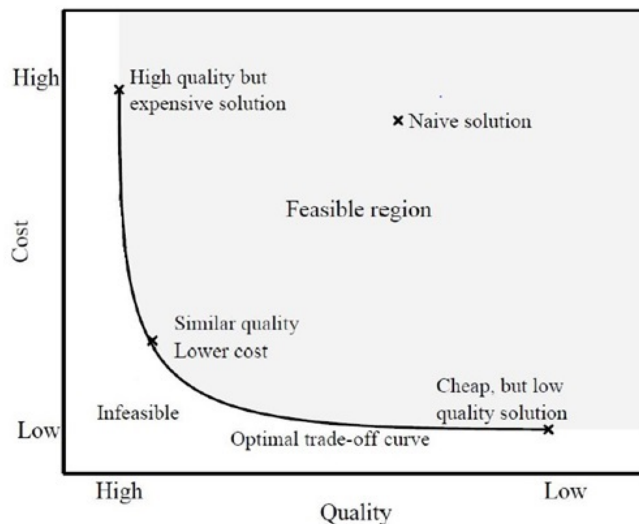
Figure 3.7: Illustration of a typical pareto curve [87]

step so that the newly created population can be integrated with the old population while maintaining the preference for the more suitable, child, solutions that have been generated [86].

3.8.1 Design Variables and Objectives

BESS/Gen Model

For both configurations, it was decided that in order to achieve a conflicting trade-off the two optimization objectives should be: to minimize the amount of carbon dioxide emitted by the power plant and to minimize the FFR tendered price that the plant can receive and still meet its financial goals. These objectives are conflicting for the fact that the natural gas generators are the cheaper technology, so using them will enable the plant to receive less compensation and still pay off the initial investment in the same amount of time. However, from an environmental impact perspective the generators produce CO_2 during their operation whereas the batteries have no emissions during the use phase of their life cycle.

The variables that were chosen to be altered were the installed capacity of the batteries in MWh, the installed capacity of the generators in MW, and the minimum acceptable SOC level for the batteries during daily operation (excluding when providing FFR services).

44

PV/BESS/Gen Model

The two design objectives stayed the same in this configuration for the reasons detailed earlier; the addition of the photovoltaic modules doesn't affect things since PV is more expensive than the gensets yet produces no emissions. The chosen variables also remained the same with one addition, which is that the optimization alters the installed capacity of PV in MW.

Chapter 4

Results and Discussion

4.1 Solutions

4.1.1 Generator Stand-alone (Gen-SA) Solution

One of the main issues with using the generators in a standalone capacity is the requisite of keeping them running 100% of the time in order to meet the fast response requirements of the FFR market. Keeping the generators running all the time increases the fuel consumption nearly 100-fold over the BESS-Gen case examined below, and because of this the required FFR tender price is driven up so that it can cover the increased operating costs of the plant. Also, since the fuel consumption was excessive the CO_2 emissions were also elevated, which meant the UK's carbon tax (which is set at roughly 24 \$/tonne until 2021) had a much larger impact [89].

Another drawback of this option is that the increased operating hours for the equipment mandates that they have to be replaced twice during the 25-year plant lifespan, whereas the other configurations never needed generator replacements.

Examining table 4.1, it can be seen that the genset stand-alone option offers an initial investment that is the lowest among all options considered (see table 4.6), however the OPEX is nearly as large as the CAPEX (76%). A review of all

Table 4.1: Performance metrics for the gas generator stand alone simulation

Indicator	Value	Unit
Capacity	20	MW
CAPEX	7.96	mil USD
OPEX	6.04	mil USD
FFR tender prices	421.91	USD/hr
Elec. Yield	52.56	GWh
CO_2	0.70	kg/kWh
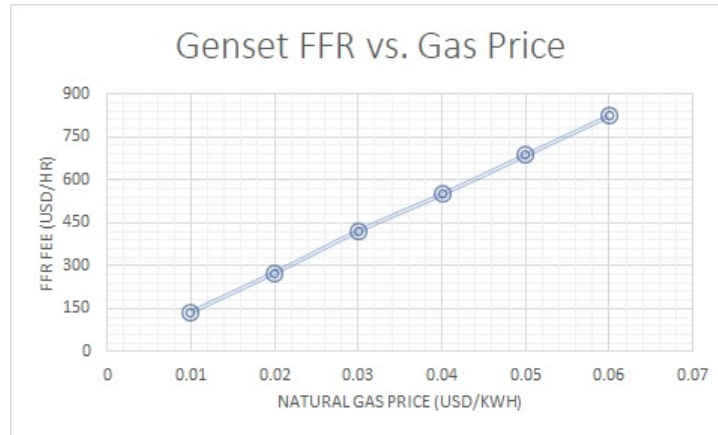
Figure 4.1: Graph portraying the relationship between the price of natural gas and the required FFR Fee of the stand alone generator plant

of the accepted tender offers (made available on the National Grid website) for 2016 established that the average FFR nomination fee for 20 MW plants was approximately 340 \$/hr [90]. So, although this option could still potentially compete with current FFR service providers, it is very vulnerable to the sensitivity of the natural gas market, which only stands to increase in the coming years [88]. Figure 4.1offers a small visualization is given which depicts how the FFR tender price is affected by changes in the natural gas price.

4.1.2 BESS-Gen Solution

For this configuration, a multi-variable optimization was performed to help isolate which combinations of battery and gas generator technology would prove to be the most economical and environmentally friendly. Surveying graphs 4.2a and 4.2b, each one of the points represents a different configuration of BESS-Gen power plant. Taking into consideration that the IRR was held constant, at a value equal to the WACC, it can then be understood that any one of these data points is equally as profitable as the next. It can be noticed that there are two points (indicated with the letter "D" and "X" sitting just to the right of each one, respectively) which achieved very similar values of FFR tender fee required for the plant, 62.26 and 63.21 \$/hr, respectively. However, points D and X have rather different design characteristics, which are detailed further in table 4.2.

The graphs (4.2a and 4.2b) also confirm the notion that as the CAPEX of each individual increases it needs to seek a higher FFR tender price so that it earn sufficient revenue to cover the investment costs.

Even though a multi-objective optimization process was utilized in this simulation, the resulting graphs do not exhibit the typical pareto curve which might be expected. There are a few factors that could explain why this was the case.
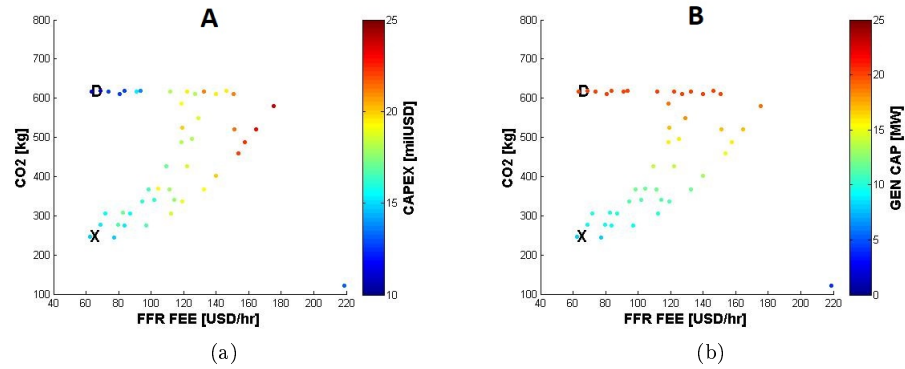
Figure 4.2: Results from the multi-variable optimization of the BESS-Gen power plant configuration which sought to minimize both FFR tender bid price and CO_2 emissions: Figure A shows data points representing the CAPEX values of each different configuration attempted during the optimization process and Figure B has data points depicting the generator capacity of each different configuration. In each figure point "D" symbolizes the solution BESS-Gen #1 and point "X" symbolizes the alternative solution BESS-Gen #2.

For one thing, certain guidelines for participation in the FFR market stipulate that if a service provider fails to provide regulation services more than three times in one month, the contract can potentially be terminated. In order to help the simulation isolate and eliminate plants which did not meet the FFR requirements, if a plant had any month(s) with more than three failed frequency responses, it would lose the FFR revenue for that month plus face an additional three month penalty (this additional penalty is not based on any information provided by National Grid, it is just a device that would help to eliminate bad plants from the simulation). The second factor that has distorted the shape of the data points on the graph is line of points at the top which all have 20 MW of installed gas generator capacity. Operationally these points are a bit different than the others with the reason being that as a whole, each plant is designed to offer 20 MW of electricity production and while also providing both primary and secondary frequency response services. If a plant has 20 MW of genset capacity, then it has no trouble to provide the full 20 MW for the entire 30 minutes required from secondary response providers, however, any plant with less than 20 MW of gensets needs the batteries to provide the additional production during this time, which sometimes is not possible if the battery system lacks the requisite charge.

From first glance it may appear that configuration BESS-Gen #1 is better suited for the needs of Lark Energy since it requires $3.75 million less in CAPEX and has slightly lower (44,000 $/year) operating costs, yet this would assume that things like the price of natural gas or batteries stays the same. Pursuant to gaining a better understanding of how these plants could become more or less

Table 4.2: Characteristics and financial metrics for the BESS-Gen plants (BESS-Gen #1 and BESS-Gen #2)

Indicator	BESS-Gen #1	BESS-Gen #2	Unit
Battery Capacity	5	20	MWh
Gen Capacity	20	8	MW
CAPEX	11.04	14.79	mil USD
OPEX	0.286	0.328	mil USD
FFR tender prices	63.21	62.26	USD/hr
Elec. Yield	2.46	5.55	GWh
CO_2	0.25	0.04	kg/kWh

Table 4.3: Table portraying the relationship between minimum allowable battery state-of-charge and electricity revenue

Min. Bat SOC [%]	Lifetime Bat Cycles [#]	FFR Fee [$/hr]	Non-Resp.	Elec. Revenue [$]
20	14375	264.05	34	646,430
30	14075	62.26	15	555,890
40	13775	69.24	4	475,920
50	13475	77.27	-	402,900

favorable moving forward they will be analyzed in greater detail in section 4.3.

One last variable that was modified during the course of the optimization process was the minimum allowable SOC of the batteries during the course of daily operation. The optimization proved that based on the current dispatch strategy of only discharging the batteries during the low frequency events or the max daily price hour, raising the minimum SOC didn't help to reduce the number of battery cycles in a significant way and it had a negative effect on the revenue from wholesale electricity market. At the same time, these modifications did reveal that the plant's reliability in providing FFR services increased as the minimum allowable SOC was raised.

Reflecting upon the findings in table 4.3, it can be seen that raising the minimum SOC does not reduce the total battery life cycles enough to compensate for the lost revenue from electricity sales. However, it is beneficial to increase the minimum SOC to 30% so that the number of frequency response unavailabilities gets reduced to an acceptable level.

4.1.3 PV-BESS-Gen Solution

The PV modules were added into the configuration with the hopes of reducing the systems reliance on the natural gas-fired generators, to reduce the amount of electricity purchased from the grid to charge the batteries, and to increase the electricity that could be generated and sold. However, after the model was constructed and the simulations were carried out it became evident that this
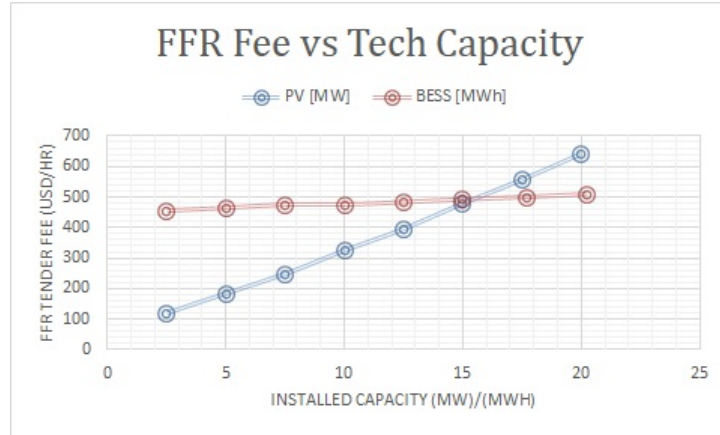
Figure 4.3: Graph illustrating how altering the PV capacity or the BESS capacity, while holding other capacities constant, can affect the required FFR tender fee

Table 4.4: Plant characteristics of the optimal PV-BESS-Gen configuration

Indicator	Value	Unit
PV Capacity	1.25	MW
Battery Capacity	2.5	MWh
Gen Capacity	19	MW
CAPEX	12.42	mil USD
OPEX	0.253	mil USD
FFR tender prices	81.72	USD/hr
Elec. Yield	4.01	GWh
CO_2	0.14	kg/kWh

was not the case. In figure 4.3, the results of 16 different simulations are shown. In 8 of the simulations the installed PV capacity was varied while the values of BESS and gensets was held at 10 MWh and 15 MW, respectively, and then in the other 8 simulations the BESS capacity was changed while the PV and gensets were set at 15 MW each. The graph clearly indicates that a reduction in the PV capacity has a much larger impact on the necessary FFR tender fee than a reduction in battery capacity.

With regards to eliminating the need for gas generators, the PV doesn't pass the test, due to a lack of reliability in production. The best that could be achieved was reducing the genset capacity to 2 MW, which required 20 MW of installed PV and 20 MWh of BESS and the plant then needed a FFR tender fee of 620.36 $/hr. Thus, through optimization the most economical system was determined and its characteristics can be seen in table 4.4.

Regarding the PV capacity, 1.25 MW was chosen because it is size of one

Table 4.5: Summary of the characteristics of the chosen BESS stand alone plant

Indicator	Value	Unit
Battery Capacity	32.5	MWh
CAPEX	18.9	mil USD
OPEX	0.130	mil USD
FFR tender prices	76.50	USD/hr
CO_2	-	tonnes

of the arrays utilized in the Lark Energy solar farm located in the UK, and the production data provided by the company listed the DC output of each array of the farm in 15 minute intervals.

One final operational theory that was proved to be false was the belief that adding the PV modules to the configuration would save the plant money by enabling it to charge the batteries for free. In the UK the average minimum daily electricity price is 36.16 \$/MWh, so with the batteries charging from the PV once per day for the entire year the savings generated are approximately \$33,000. This number is not only too small of a percentage of the CAPEX (only 1.1%) to lead to payback in the 25-year plant lifespan, it is only 19% larger than the OPEX costs for the PV system (27,637 \$/year). Raising the PV and battery capacity does lead to additional savings, but the ratio of savings to OPEX actually decreases (for a system with 20 MW of PV and 20 MWh of batteries, \$263,968 is saved compared with a PV OPEX of 474,580 \$/year).

4.1.4 Battery Bank Stand-alone (BESS-SA) Solution

The last configuration that was attempted was one that which only implemented batteries to perform energy arbitrage while also participating in the FFR and capacity markets. There was no need to perform an multi-objective optimization for this since there were not a vast amount of variables to alter. Considering the fact that the batteries in this configuration did not have the reliability of the generators to help shoulder the load of frequency response services, it was necessary to oversize the installed capacity of the batteries so that their participation in both markets would not be jeopardized. Figure 4.4 illustrates how additional battery capacity reduces the number of non-responses (Non-Resp) to low frequency events committed by the system.

As explained earlier, more than three non-responses in a month will result in a penalty and drive up the FFR tender fee that the plant must seek; in the graph the lowest three battery capacities (22.2, 25.2, and 27.8 MWh) all receive penalties for two months, the 30.4 MWh plant is penalized in one month, and the highest three battery capacities (32.9, 35.4, and 38 MWh) are reliable enough to where they do not incur any penalty. From the graph, the plant with the lowest required FFR tender fee was chosen as the best option, and additional information about this plant can be seen in table 4.5.
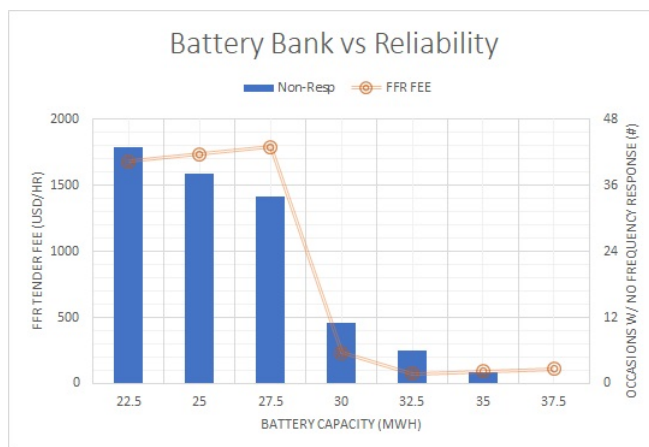
Figure 4.4: Graph portraying the relationship between installed battery capacity and the number of times the plant fails to provide FFR services, as well as the FFR tender fee the plant must charge

Table 4.6: Comparison of results for the different power plant configurations

Model	CAPEX	OPEX	FFR price	CO_2
Gen-SA	7.96	6.04	421.91	0.70
BESS-Gen (1)	11.05	0.286	63.22	0.25
BESS-Gen (2)	14.79	0.328	62.26	0.04
PV-BESS-Gen	12.42	0.253	80.59	0.14
BESS-SA	18.89	0.130	76.5	-

4.2   Comparison

Having reviewed the four potential configurations that can be used to effectively participate in multiple markets in the UK, a comparison can now be made to see how they stack up against one another. All of these plants have IRRs of 12% and use the same initial economic parameters, so they are equally profitable, what differentiates them most is how much initial investment they require and how much they need to be compensated for providing FFR services. Analyzing table 4.6, it can be seen that the first option of using only generators does provide the lowest CAPEX value, but is the worst in every other category. The two BESS-Gen options offer the lowest FFR tender fees and have CAPEX values that fall in the middle of the range. The BESS stand-alone option has the highest CAPEX but with the recent plummet of lithium-ion battery prices signaling a bright future for battery storage it would be good to analyze this configuration in a sensitivity analysis.

From this table, three were selected to be analyzed under the conditions of a sensitivity analysis (BESS-Gen #1, BESS-Gen #2, and BESS-SA).
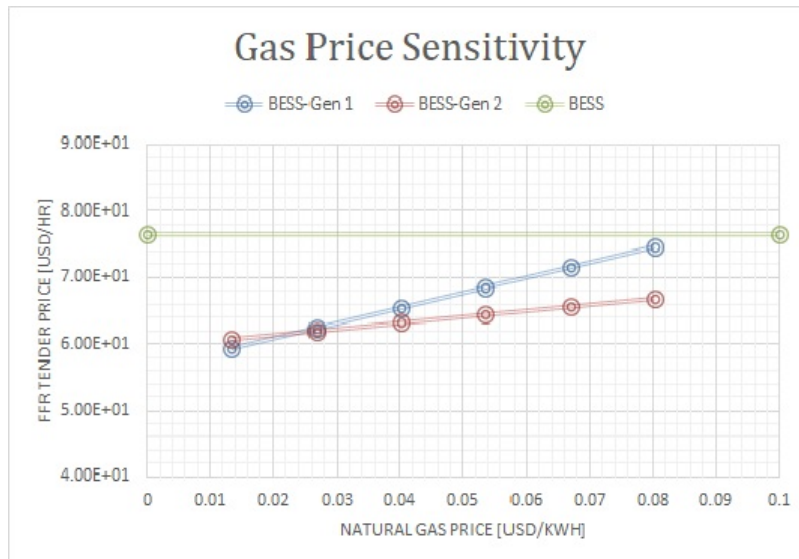
Figure 4.5: Sensitivity analysis to examine how changes in the natural gas price affects the FFR tender that each plant must charge

4.3 Sensitivity

The three parameters that were decided upon for the purposes of a sensitivity analysis are the price of natural gas (in $/kWh), the investment cost of lithium-ion batteries (in $/kWh), and the wholesale electricity price (in $/MWh). The gas price was chosen because natural gas make up a fair portion of the OPEX for the two configurations of BESS-Gen hybrid plants and as history has shown, the natural gas price is subject to change as market conditions have varied. The price of batteries is interesting because in the past several years, thanks to the help of companies like Tesla and others, batteries prices reduced to less than 50% of their previous value [93]. Finally the electricity price is good to analyze since it is predicted to vary over the coming years as generational resouces change.

4.3.1 Gas Price Sensitivity

The natural gas price used for the simulations was found to be 0.029 $/kWh (converted from 0.025 EUR/kWh) [91]. It can be seen by examining figure 4.5 that as the gas price increases it clearly makes BESS-Gen #2 the more desirable configuration. Analyzing the previous eight years of natural gas price data for the European Union (see Appendix B.1), it can be seen that the variance in the gas price ranges from 0.3 - 0.48 and has been on a downward trend in the past three years, with the UK's prices being assumed to be slightly lower than the EU average based on the 2016 data [92, 91]. It does not seem like changes to the gas price alone will make the stand alone BESS the cheapest option, because
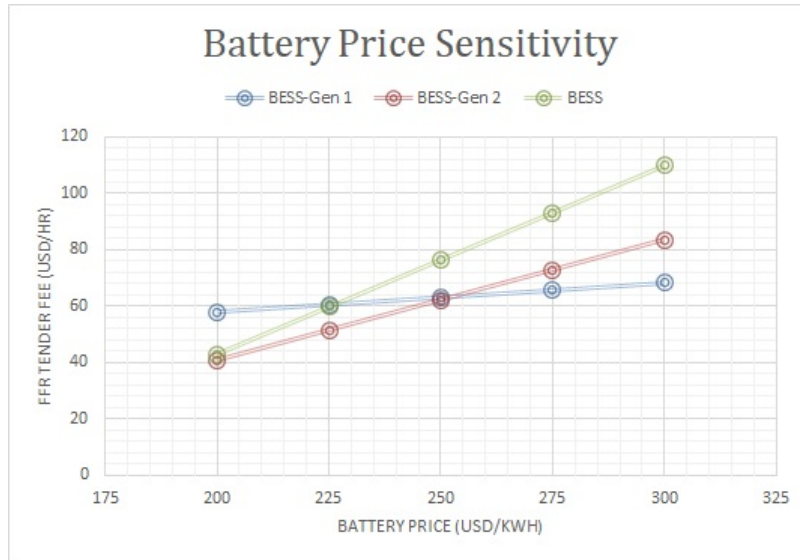
Figure 4.6: Sensitivity analysis to examine how changes in the market price of batteries would allow for changes in the FFR tender fee of each plant

even if the natural gas price triples, which is very unlikely given historical trends and current market standing, the BESS is still in last place among the three options.

4.3.2 Battery Price Sensitivity

Examining figure 4.6, it can be seen that at the current price of 250 $/kWh the two BESS-Gen configurations are nearly identical in price, but as the price of batteries decreases configuration #2 becomes more attractive. Another observation is that the stand alone BESS configuration is the most sensitive to the battery price. A 10% reduction in battery price makes the BESS-SA equal to BESS-Gen #1, and with a 20% reduction in battery price it is able to pull even with BESS-Gen #2. The CAPEX of the BESS only option also becomes more competitive with the other two options as the battery costs are reduced; for a battery price of 200 $/kWh the CAPEX falls to $16.1 million, whereas the CAPEX of the BESS-Gen #2 reduced by a smaller margin to $13.1 million. In a report made by Bloomberg technology, they summarized the surveys for industry prices of Lithium-Ion batteries from 2013 to 2016 and showed that the prices have fallen from around 600 $/kWh to around 275 USD/kWh [93]. For the industry prices to have dropped by over 50% in 4 years, it is reasonable to project them falling to 200 $/kWh or lower in the coming few years, meaning stand alone battery banks will become increasingly utilized.
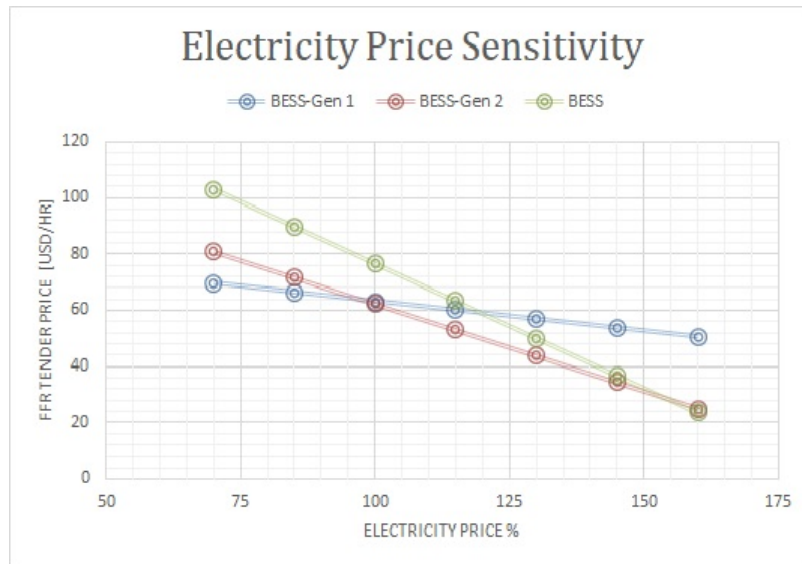
Figure 4.7: Sensitivity analysis to examine how percentage variations in the electricity price (100% is present value) determine the FFR tender fee for each plant

4.3.3 Electricity Price Sensitivity

The sensitivity analysis for the electricity price (figure 4.7) was performed by adjusting the hourly electricity used in the simulation by a percentage multiplier. That is to say, 100% represents the actual electricity prices used in the model, any data points to the right represent an assumed overall increase in electricity prices and the data points to the left of 100% represent a decrease in prices. One trend that the analysis illustrates is the fact that the configurations which contain higher installed battery capacities are more sensitive to changes in the electricity prices. This trend is present because the more battery capacity a plant has the more it is able to provide electricity arbitrage to the market. Reviewing projections and future assumptions made by the UK government, it can be seen that they expect the wholesale electricity prices to grow in the coming years; estimating a 11% growth by 2020 and as much as a 39% growth over current prices by 2024 (see Appendix B.2) [94].

4.4 Discussion

For a company to make a large multi-million dollar investment into a power plant that they intend on using for the next 20 to 25 years, the decision makers need to assess market conditions not only as they are in the present but as well how they are going to shift and evolve in the years to come. If one were to be forced

Table 4.7: Table depicting a potential implementation strategy for a hybrid plant which would account for changing market conditions moving forward

Parameter	2017	2023
Battery Price [$/kWh]	250	200
Electricity Price [%]	100	130
Battery CAPEX [milUSD]	11.6	6.2
Genset CAPEX [milUSD]	3.2	-
Required FFR Fee [$/hr]	62.26	53.36
Tendered FFR Fee [$/hr]	150	53.36
Additional Revenue [$/yr]	791440	-

to choose power plant configuration based solely upon present market prices and conditions they would probably opt for the BESS-Gen #1 configuration since it offers the best current combination CAPEX and FFR tender fee. However, when taking into account the trends of battery prices and electricity price in the coming years, it would be a wiser choice to opt for the BESS-Gen #2 option or even the BESS-SA option.

One possibility for a company like Lark would be to construct and operate the BESS-Gen #2 power plant for a few years, and if they were to bid into the FFR market at a tender price higher than necessary they could make additional revenue that would allow them to quickly pay off the investment in the gas generators. Then, having paid off the gas generators, they could remove them from the configuration and transition to a BESS-SA plant at a point in time when the battery price had dropped enough to make this system cost-competitive. To give this plan more concrete data, table 4.7 was constructed to breakdown the costs and implementation strategy.

The calculations for 2023 were made assuming that the battery price has reduced to 200 $/kWh and the electricity price will have increased to 130% of its current value, as predicted by market research [94, 93]. The simulation was run for a plant lifetime of 20 years, instead of 25 years which was used for all other cases. The new FFR tender price of 53.36 $/hr would be a slight improvement over the 62.26 $/hr required by the BESS-Gen #2, and considering the economic calculations were made assuming a constant FFR tender price (accounting for inflation) over the plant's lifespan, it is a competitive advantage for the plant owners if they are able to reduce their required compensation midway through the lifespan.

Chapter 5

Conclusions

Now that the completed work has been detailed and elaborated above, it is time to conclude with a brief summary of what took place during the course of this thesis, what accomplishments were made, and how the research could potentially be extended and enhanced moving forward. Before moving ahead to the Achievements section, it is important to first reflect upon the objectives that were specified at the beginning of the report. The main objective for the work was to determine what type of hybrid plant (technology and capacity-wise) should a developer seek to build that will be able to participate in three electricity-centric markets (the wholesale electricity market, Firm Frequency Response services market, and the capacity market) while being financially optimal. This goal was accomplished through a multitude of steps, which are enumerated in the following section.

5.1 Achievements

The initial goal that was carried out was the performance of a thorough literature review which uncovered good deal of related research that helped to provide support for this thesis while at the same time allowing it to differentiate itself from the others. The literature review also examined the current state of the art for technologies which were simulated and also studied some additional hybridization schemes found in previous research. Secondly it was essential for the existing software and simulation tools to be studied and thoroughly comprehended so that any discrepancies of functional capabilities could be determined and alleviated. Next came one of the more important achievements, the creation of two new models in the DYESOPT tool. These models allowed for the simulation of two separate power plant configurations (a combined BESS-Gen hybrid plant and a PV-BESS-Gen hybrid plant) which were not previously part of DYESOPT's capabilities. Beyond the results themselves, these two models were probably the most important achievement that was made during the course of this thesis work. Their creation required countless of hours

coding, debugging, several consultations of the online help database, postulating and validating theories, until finally the models were functional.

With these new models in place, simulations were performed to so that the valid combinations of the batteries, generators and PV modules could be discovered. At this point an optimization routine was run which highlighted a few superior configurations (two BESS-Gen plants and one BESS stand-alone plant) of the power plant and also specified the FFR tender price that this plant must obtain in order to meet its financial goals. The first potential solution (BESS-Gen #1) was composed of 20 MW of gas generators and 5 MWh of Li-Ion batteries, had a CAPEX of \$11.05 million and required a FFR tender bid of 63.22 \$/hr. The second viable solution (BESS-Gen #2) consisted of 8 MW of gas generators and 20 MWh of Li-Ion batteries, its CAPEX was 34% higher than BESS-Gen #1 and it needed an FFR tender that was only 1.5% lower. Lastly, the final solution considered was a battery bank stand-alone plant with 32.5 MWh of installed capacity, its CAPEX was 71% higher and its required FFR tender was 21% higher. The reason that the latter two solutions were not overlooked in favor of BESS-Gen #1 was for the fact that parameters, such as electricity and gas price, stand to change in the coming years, thus changing the economic outlook of each solution. Finally, in order to further evaluate and quantify which potential plant type would offer the best selection moving forward a sensitivity analysis was performed based on these research predicted changes to market conditions. Research suggests that the in the years to come, the price of natural gas will increase, the price of Li-Ion batteries will decrease, and the price of electricity in the UK will increase. Under each one of these projections, the BESS-Gen #2 configuration improves in comparison with BESS-Gen #1. Also, in order for the BESS stand-alone system to outperform BESS-Gen #1, with regards to FFR tender fee, it would only require a 21% drop in the price of batteries or a 20% increase in the average hourly electricity price.

5.2   Future Work

The following are some areas in which the work carried out in this thesis could be expanded upon and possibly improved:

- It would be wise to investigate the implementation of batteries with different charge and discharge rates. It would be interesting to analyze how a variation of these charge/discharge rates could potentially affect the dispatch strategy and in the long term, the total revenue for the plant.

- This simulation only accounts for the current conditions existing in the United Kingdom, it would be good practice to assess the viability of such a system in different markets. For instance, currently in the U.K. there are no subsidies for the installation of renewable energy based technology, so studying a country that offered such subsidies would be interesting.

- One last change that could be made would be to make alterations to the battery bank stand-alone configuration. It would intriguing to see if a system that consisted of two battery banks (each having the ability to independently charge, discharge or remain idle as the controller dictated) could provide more reliable and optimal grid regulation services. This possibility will become increasingly interesting as the price and longevity of grid-scale battery systems continues to improve.

Bibliography

[1] Neslen, A. (2016, May 18). Portugal runs for four days straight on renewable energy alone, available at https://www.theguardian.com/environment/2016/may/18/portugal-runs-for-four-days-straight-on-renewable-energy-alone, accessed on 15/2/2017

[2] Masters, G. M. (2013). Renewable and efficient electric power systems (2nd ed.). Wiley.

[3] National Grid (2015, December). Firm Frequency Response: Frequently Asked Questions, available at http://www2.nationalgrid.com/WorkArea/DownloadAsset.aspx?id=44429, accessed on 16/2/2017

[4] National Grid (2017). Capacity Market, available at https://www.emrdeliverybody.com/cm/home.aspx, accessed on 19/5/2017

[5] Paterakis, N. G. (2017). Optimal Procurement of Contingency and Load Following Reserves by Demand Side Resources Under Wind-Power Generation Uncertainty. Optimization in Renewable Energy Systems, 75-116.

[6] PWC (2017). Managing a revenue downturn while meeting the demands of consumers, available at https://www.strategyand.pwc.com/media/file/2017-Power-and-Utilities-Industry-Trends.pdf, accessed on 2/9/2017

[7] Black, M., (2006). Value of storage in providing balancing services for electricity generation systems with high wind penetration. Journal of Power Sources, vol. 162(2), 949-953

[8] Byrne R. H. (2012). Estimating the Maximum Potential Revenue for Grid Connected Electricity Storage: Arbitrage and Regulation: A Study for the DOE Energy Storage Systems Program, Sandia National Laboratories, Albuquerque, New Mexico, USA

[9] Rasmussen, M. G. (2012). Storage and balancing synergies in a fully or highly renewable pan-European power system. Energy Policy, 51, 642-651

[10] Ortega-Vazquez, M. A. (2014). Optimal scheduling of electric vehicle charging and vehicle-to-grid services at household level including battery degradation and price uncertainty. IET Generation, Transmission & Distribution, vol. 8(6), 1007-1016

[11] Eto, J. H. (2010). Use of Frequency Response Metrics to Assess the Planning and Operating Requirements for Reliable Integration of Variable Renewable Generation, available at https://www.ferc.gov/industries/electric/indus-act/reliability/frequencyresponsemetrics-report.pdf, accessed on 17/2/2017

[12] Mokrian, P. (2006). A Stochastic Programming Framework for the Valuation of Electricity Storage, available at http://www.iaee.org/en/students/best_papers/PedramMokrian.pdf, accessed on 17/2/2017

[13] Olatomiwa, L. (2015). Economic evaluation of hybrid energy systems for rural electrification in six geo-political zones of Nigeria. Renewable Energy, vol. 83, 435-446

[14] Baneshi, M. (2016). Techno-economic feasibility of hybrid diesel/PV/wind/battery electricity generation systems for non-residential large electricity consumers under southern Iran climate conditions. Energy Conversion and Management, vol. 127, 233-244

[15] Tsuanyo, D. (2015). Modeling and optimization of batteryless hybrid PV (photovoltaic)/Diesel systems for off-grid applications. Energy, vol. 86, 152-163.

[16] Castillo, L. (2014). Techno-economic Analysis of Combined Hybrid Concentrating Solar and Photovoltaic Power Plants: A Case Study for Optimizing Solar Energy Integration into the South African Electricity Grid, KTH, Stockholm

[17] Larchet, K. (2015). Solar PV-CSP Hybridisation for Baseload Generation: A Techno-economic Analysis for the Chilean Market, KTH, Stockholm

[18] Hansson, L. (2016). Impact of Time-of-Delivery Schemes on Optimum Solar Hybrid Power Plants: A Techno-Economic Study, KTH, Stockholm

[19] Staffel, I. (2016). Maximising the Value of Electricity Storage, Journal of Energy Storage, 8, 212-225

[20] Kumbartzky, D. (2017). Optimal operation of a CHP plant participating in the German electricity balancing and day-ahead spot market, European Journal of Operational Research, vol. 261, 390-404

[21] Amaral, A.M. (2017, October 25). Solar Cell Fundamentals, pg. 15-19. Lecture presented at Photovoltaic Solar Energy (ESF-2) in IST, Lisbon

[22] Ferreira de Jesus, J. M. D., (2016, November 15) Equivalent Circuit Diagrams of Photovoltaic Modules, pg. 10-16, 21-26, 29-31. Lecture presented at Photovoltaic Solar Energy (ESF-2) in IST, Lisbon

[23] Rodrigues, E. (2011). Simulation of a solar cell considering single-diode equivalent circuit mode. Renewable Energy and Power Quality Journal, 369-373

[24] Sandia National Labs. (2017). Single Diode Equivalent Circuit Models, available at https://pvpmc.sandia.gov/modeling-steps/2-dc-module-iv/diode-equivalent-circuit-models/, accessed on 16/10/2017

[25] IRENA (2016). Renewable Energy Statistics 2016, available at http://www.irena.org/DocumentDownloads/Publications/IRENA_RE_Statistics_2016.pdf, accessed on 20/2/2017

[26] Vartiainen, E. (2017, February 13). Solar energy technologies, markets and competitiveness. Lecture presented at Large Scale Solar Power (MJ2500) in KTH, Stockholm.

[27] IEA, (2016). Energy, Climate Change and Environment: 2016 Insights, available at www.iea.org/publications/freepublications/publication/ECCE2016.pdf, accessed on 16/2/2017

[28] Montemor, F. (2016, November 24). Energy Storage: Secondary Batteries, presented at Energy Storage in Instituto Superior Tecnico, Lisbon.

[29] Montemor, F. (2016, November 24). Energy Storage: Li Ion Batteries, presented at Energy Storage in Instituto Superior Tecnico, Lisbon.

[30] Huggins, R. A. (2010). Energy storage. New York: Springer.

[31] Ambri (2016) Ambri Brochure, available at http://www.ambri.com/technology/, accessed on 23/2/2017

[32] Sadoway, D. (2012) The Missing Link to Renewable Energy, presented at TED2012 in Long Beach, California

[33] Montemor, F. (2016, November 24). Energy Storage: Primary Batteries, presented at Energy Storage in Instituto Superior Tecnico, Lisbon.

[34] EOS (2017). EOS Aurora 250/1000 System Specification, available at http://www.eosenergystorage.com/products/, accessed on 23/2/2017

[35] Soloveichik, G. L. (2015). Flow Batteries: Current Status and Trends. Chemical Reviews, vol. 115(20), 11533-11558.

[36] Xing, X. (2011, November 25). Vanadium Redox-Flow Battery, available at http://large.stanford.edu/courses/2011/ph240/xie2/, accessed on 17/10/2017

[37] Boquiang, L. (2017). Economic viability of battery energy storage and grid strategy: A special case of China electricity market. Energy, vol. 124, 423-434.

[38] Kokam (2015, November 2). Kokam ESS Proposal: Prelimary Proposal prepared for Lark Energy

[39] Zakeri, B. (2015) Electrical energy storage systems: A comparative life cycle cost analysis, Renewable and Sustainable Energy Reviews, vol. 42

[40] Kear, G. (2011). Development of the all-vanadium redox flow battery for energy storage: a review of technological, financial and policy aspects. International Journal of Energy Research, 36(11), 1105-1120.

[41] Bach, T. C. (2016). Nonlinear aging of cylindrical lithium-ion cells linked to heterogeneous compression. Journal of Energy Storage, vol. 5, 212-223

[42] Wankmüller, F. (2016). Impact of battery degradation on energy arbitrage revenue of grid-level energy storage. Journal of Energy Storage, vol. 10 (2017), 56-66

[43] Haaren, R. V. (2015). An energy storage algorithm for ramp rate control of utility scale PV (photovoltaics) plants. Energy, vol. 91, 894-902

[44] Bullich-Massagué, E. (2017) Active power control in a hybrid PV-storage power plant for frequency support, Solar Energy, vol. 144, 49-62

[45] Dufo-López, R. (2014). Comparison of different lead–acid battery lifetime prediction models for use in simulation of stand-alone photovoltaic systems. Applied Energy, 115, 242-253

[46] Duda, M. (2017, February 15). Cummins Power Systems: Gas Generator Sets. Presentation made to Lark Energy office in Bourne, United Kindom

[47] Cummins, (2014). PowerCommand 3300 Control Panel, available at https://cumminsengines.com/brochure-download.aspx?brochureid=357, accessed on 16/3/2017

[48] Cummins. (2010, May 25). Diesel generator set QSK60 series engine - Specification Sheet, pp. 24-31, available at www.globalpwr.com/wp-content/uploads/cut-sheets/cummins-dqkab-1535.pdf, accessed on 2/3/2017

[49] Rezzouk, H. (2015). Feasibility study and sensitivity analysis of a stand-alone photovoltaic–diesel–battery hybrid energy system in the north of Algeria. Renewable and Sustainable Energy Reviews, vol. 43, 1134-1150

[50] Adaramola, M. S. (2014). Assessment of decentralized hybrid PV solar-diesel power system for applications in Northern part of Nigeria. Energy for Sustainable Development, vol. 19, 72-82

[51] Clean Horizon (2013, September 8). Frequency Regulation: The Need for Fast Responding Assest and the Mileage Case in the USA, available at http://www.cleanhorizon.com/blog/2013/09/frequency-regulation-the-need-for-fast-responding-assets-and-the-mileage-case-in-the-usa/, accessed on 29/8/2017

[52] Boston University (1999). Rotational kinetic energy and angular momentum, available at http://physics.bu.edu/~duffy/py105/AngularMo.html, accessed on 1/9/2017

[53] National Grid (2017). Firm Frequency Response (FFR), available at http://www2.nationalgrid.com/UK/Services/Balancing-services/Frequency-response/Firm-Frequency-Response/, accessed on 16/2/2017

[54] ESA. (2017). Spinning Reserve, available at http://energystorage.org/energy-storage/technology-applications/spinning-reserve, accessed on 17/10/2017

[55] IEC, (2017). World Plugs, available at http://www.iec.ch/worldplugs/map.htm, accessed on 15/3/2017

[56] Thinking Grids, (2015). Commercial Frequency Response Market Worth £126M in 2014/2015, available at http://www.thinkinggrids.com/ancillary-services/commercial-frequency-response-market-worth-126m-in-2014-2015, accessed on 13/2/2017

[57] National Grid (2016). Summer Outlook Report, available at http://www2.nationalgrid.com/UK/Industry-information/Future-of-Energy/FES/summer-outlook/, accessed on 28/02/2017

[58] Ofgem. (2015, September 09). The GB electricity wholesale market available at from https://www.ofgem.gov.uk/electricity/wholesale-market/gb-electricity-wholesale-market, accessed on 7/9/2017

[59] NordPool (2017). Market data: N2EX Day Ahead Auction Prices, available at http://www.nordpoolspot.com/Market-data1/GB/Auction-prices/UK/Hourly/?view=table, accesssed on 5/3/2017

[60] National Grid (2016, June 2). Enhanced Frequency Response Seminar, available at http://www2.nationalgrid.com/Enhanced-Frequency-Response.aspx, accessed on 13/2/2017

[61] Curtis, M. (2015, September 11). Overview of the UK Demand Response Market. Lecture presented at EPFL Workshop, in the University of Reading, Berkshire, UK

[62] James, A. (2013, June 3). How a Capacity Market Works, available at http://www.theenergycollective.com/adamjames/237496/energy-nerd-lunch-break-how-capacity-market-works-and-why-it-matters, accessed on 20/5/2017

[63] Topel, M. (2015, February 2) "Modeling Tools," KTH, Available: https://www.kth.se/en/itm/inst/energiteknik/forskning/kraft_varme/ekv-researchgroups/csp-group/modeling-tools-1.493747, accessed on 17/2/2017

[64] Resources, E. (2017). TRNSYS. available at http://www.trnsys.com/, accessed on 10/9/2017

[65] Sulaiman, S. (2011). Sizing Grid-Connected Photovoltaic System Using Genetic Algorithm, in Symposium on Industrial Electronics and Applications, Langkawi

[66] Mattei, M. (2006). Calculation of the polycrystalline PV module temperature using a simple method of energy balance, Renewable Energy, vol. 31, 553-567

[67] M. Almaktar, M. (2013). Climate Based Empirical Model for PV ModuleTemperature Estimation in Tropical Environment, Applied Solar Energy, vol. 49, no. 4, 192-201

[68] Shepherd, C. (1965). Design of Primary and Secondary Ceils II: An Equation Describing Battery Discharge, Journal of Electrochemical Society, vol. 112, no. 7, 657-664

[69] Battery University, (2015). Basics About Discharging, Battery University, available at http://batteryuniversity.com/learn/article/discharge_methods, accessed on 4/3/2017

[70] Kurt, D. (2016, April 25). Net Present Value - NPV, available at http://www.investopedia.com/terms/n/npv.asp, accessed on 5/9/2017

[71] Picardo, C. E. (2014, January 23). Discount Rate, available at from http://www.investopedia.com/terms/d/discountrate.asp, accessed on 5/9/2017

[72] Staff, I. (2017, September 01). Internal Rate Of Return - IRR, available at http://www.investopedia.com/terms/i/irr.asp, accesssed on 5/9/2017

[73] Staff, I. (2015, September 29). Weighted Average Cost of Capital - WACC, available at http://www.investopedia.com/terms/w/wacc.asp, accesssed on 5/9/2017

[74] US-DOE. (2015, August 25). Levelized Cost of Energy (LCOE). Lecture, available at https://energy.gov/sites/prod/files/2015/08/f25/LCOE.pdf, accessed on 5/9/2017

[75] WACC Expert (2017). United Kingdom - Technology, available at http://www.waccexpert.com/, accessed on 5/9/2017

[76] Gov.UK. Tax on shopping and services. available at https://www.gov.uk/tax-on-shopping/energy-saving-products, accessed on 5/9/2017

[77] UK inflation rate at near four-year high. (2017, June 13) available at from http://www.bbc.com/news/business-40259392, accessed on 5/9/2017

[78] Cummings, K. (2007). Understanding physics. New Delhi: John Wiley & Sons Inc., pg. 449, 484, 485, 487

[79] Eos, (2016). Eos Aurora 250|1000 System Specification, Znyth Technology, available at http://www.eosenergystorage.com/wp-content/uploads/2017/02/eos-aurora-specification-summary_v2.pdf, accessed on 16/3/2017

[80] IEA (2017). United Kingdom - Energy Systems Overview, available at https://www.iea.org/media/countries/UnitedKingdom.pdf, accessed on 2/9/2017

[81] National Grid (2017). UK Profile, available at http://investors.nationalgrid.com/about-us/our-markets/uk-profile.aspx, accessed on 17/2/2017

[82] National Grid, (2015). Firm Frequency Response: Frequency Asked Questions, ver. 1.2, pg. 8, available at http://www2.nationalgrid.com/UK/Services/Balancing-services/Frequency-response/Firm-Frequency-Response/, accessed on 16/2/2017

[83] DOE, EPRI, (2013). Electricity Storage Handbook in Collaboration with NRECA, EPRI, Albuquerque

[84] EPRI, (2011). Energy Storage System Costs 2011 Update Executive Summary, EPRI

[85] EIA, (2016). Capital Cost Estimates for Utility Scale Electricity Generating Plants, U.S. Department of Energy

[86] Deb, K. (2011). Multi-Objective Optimization Using Evolutionary Algorithms: An introduction, Indian Institute of Technology, Kanpur

[87] Leyland, G. B. (2002). Multi-objective optimisation applied to industrial energy problems, Lousanne: EPFL

[88] Knoema, (2017). Natural Gas Prices Forecast: Long Term 2017 to 2030, available at https://knoema.com/ncszerf/natural-gas-prices-forecast-long-term-2017-to-2030-data-and-charts, accessed on 29/9/2017

[89] Reuters Staff (2016, November 23). Britain maintains carbon tax freeze until April 2021, available at http://uk.reuters.com/article/uk-britain-eu-budget-carbon/britain-maintains-carbon-tax-freeze-until-april-2021-idUKKBN13I1J9?il=0, accessed on 2/10/2017

[90] National Grid (2017). Services Reports, available at http://www2.nationalgrid.com/UK/Industry-information/Electricity-transmission-operational-data/Report-explorer/Services-Reports/, accessed on 10/3/2017

[91] Eurostat, (2017). Natural gas prices for industrial consumers, second half 2016 (EUR per kWh), available at http://ec.europa.eu/eurostat/statistics-explained/index.php/File:Natural_gas_prices_for_industrial_consumers_second_half_2016_(EUR_per_kWh)_YB17.png, accessed on 30/6/2017

[92] Eurostat, (2017). Development of natural gas prices for industrial consumers, EU-28, 2008-2016 (EUR per kWh), available at http://ec.europa.eu/eurostat/statistics-explained/index.php/File:Development_of_natural_gas_prices_for_industrial_consumers,_EU-28,_2008-2016_(EUR_per_kWh)_YB17.png, accessed on 29/9/2017

[93] Randall, T. (2017). Tesla's Battery Revolution Just Reached Critical Mass, available at https://www.bloomberg.com/news/articles/2017-01-30/tesla-s-battery-revolution-just-reached-critical-mass, accessed on 28/2/2017

[94] Gov.UK, (2017, March 15). Updated energy and emissions projections: 2016, Annex M: Growth assumptions and prices, available at https://www.gov.uk/government/uploads/system/uploads/attachment_data/file/599601/Annex-m-price-growth-assumptions.xls, accessed on 29/9/2017

Appendix A: Datasheets

A.1 Solar Module Datasheet

A.2 Lithium-Ion Battery Datasheet

A.3 Gas Generator Datasheet

YGE 60 CELL SERIES 2

ELECTRICAL PERFORMANCE

Electrical parameters at Standard Test Conditions (STC)

Module type			YLxxxP-29b (xxx=Pmax)				
Power output	P_{max}	W	260	255	250	245	240
Power output tolerances	ΔP_{max}	W	0 / +5				
Module efficiency	η_m	%	16.0	15.7	15.4	15.1	14.8
Voltage at P_{max}	V_{mpp}	V	30.3	30.0	29.8	29.6	29.3
Current at P_{max}	I_{mpp}	A	8.59	8.49	8.39	8.28	8.18
Open-circuit voltage	V_{oc}	V	37.7	37.7	37.6	37.5	37.5
Short-circuit current	I_{sc}	A	9.09	9.01	8.92	8.83	8.75

STC: 1000W/m² irradiance, 25°C cell temperature, AM1.5g spectrum according to EN 60904-3.
Average relative efficiency reduction of 3.3% at 200W/m² according to EN 60904-1.

Electrical parameters at Nominal Operating Cell Temperature (NOCT)

Power output	P_{max}	W	189.7	186.0	182.4	178.7	175.1
Voltage at P_{max}	V_{mpp}	V	27.6	27.4	27.2	27.0	26.8
Current at P_{max}	I_{mpp}	A	6.87	6.79	6.71	6.62	6.54
Open-circuit voltage	V_{oc}	V	34.8	34.8	34.7	34.6	34.6
Short-circuit current	I_{sc}	A	7.35	7.28	7.21	7.14	7.07

NOCT: open-circuit module operation temperature at 800W/m² irradiance, 20°C ambient temperature, 1m/s wind speed.

THERMAL CHARACTERISTICS

Nominal operating cell temperature	NOCT	°C	46 +/- 2
Temperature coefficient of P_{max}	γ	%/°C	-0.42
Temperature coefficient of V_{oc}	β_{oc}	%/°C	-0.32
Temperature coefficient of I_{sc}	α_{sc}	%/°C	0.05
Temperature coefficient of V_{mpp}	β_{mpp}	%/°C	-0.42

OPERATING CONDITIONS

Max. system voltage	1000V_{DC}
Max. series fuse rating	15A
Limiting reverse current	15A
Operating temperature range	-40°C to 65°C
Max. static load, front (e.g., snow)	5400Pa
Max. static load, back (e.g., wind)	2400Pa
Max. hailstone impact (diameter / velocity)	25mm / 23m/s

CONSTRUCTION MATERIALS

Front cover (material / thickness)	low-iron tempered glass / 3.2mm
Cell (quantity / material / dimensions / number of busbars)	60 / multicrystalline silicon / 156mm x 156mm / 2 or 3
Frame (material / color / anodization color / edge sealing)	anodized aluminum alloy / silver / clear / silicone or tape
Junction box (protection degree)	≥ IP65
Cable (length / cross-sectional area)	1000mm / 4mm²
Plug connector (type / protection degree)	MC4 / IP67 or YT08-1 / IP67 or Amphenol H4 / IP68

• Due to continuous innovation, research and product improvement, the specifications in this product information sheet are subject to change without prior notice. The specifications may deviate slightly and are not guaranteed.
• The data do not refer to a single module and they are not part of the offer, they only serve for comparison in different module types.

QUALIFICATIONS & CERTIFICATES

IEC 61215, IEC 61730, CE, MCS, ISO 9001:2008, ISO 14001:2004,
BS OHSAS 18001:2007, PV Cycle, SA 8000

GENERAL CHARACTERISTICS

Dimensions (L / W / H)	1640mm / 990mm / 35mm
Weight	18.5kg

PACKAGING SPECIFICATIONS

Number of modules per pallet	29
Number of pallets per 40' container	28
Packaging box dimensions (L / W / H)	1700mm / 1135mm / 1165mm
Box weight	566kg

Unit: mm
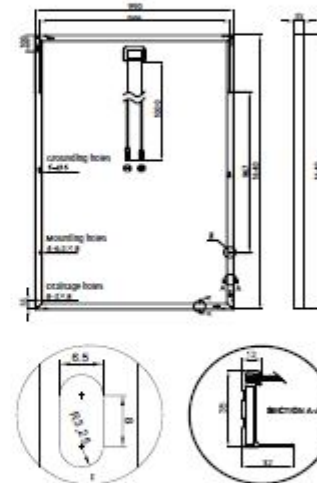
Warning: Read the Installation and User manual in its entirety before handling, installing, and operating Yingli Solar modules.

Yingli Partners:

Yingli Green Energy Holding Co., Ltd.
service@yingli.com
Tel: +86-312-2188055

YINGLISOLAR.COM

Figure A.1: Yingli 260Wp, 60 cell Solar Module Datasheet

■ **Proposed Cell:**

Model	Description
SLPB	The Superior Lithium Polymer Battery (SLPB) 75Ah cell

Front view   Side view   Elevation
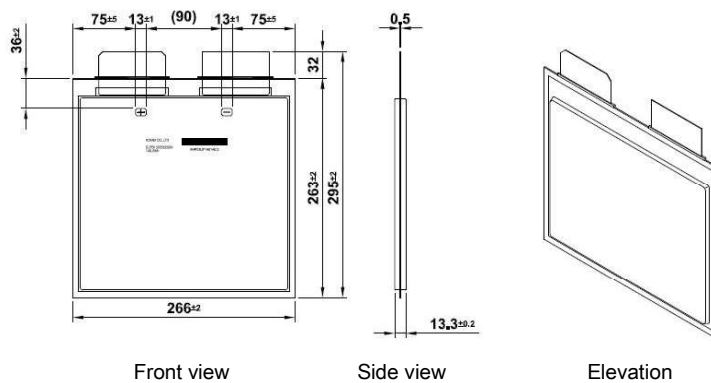
Figure 5.   Mechanical Drawing

Description		Value	Remark
Rated Capacity		≥75Ah	
Weight		1.81kg	Tab weight included
Dimension	Width	268.0mm	Unfolded
	Height	265.0mm	Tab excluded
	Thickness	13.5mm	At OCV 2.2 ±0.1V

3.3 Module

The ingenious engineering and design of Kokam's modules fully realizes the powerful potential of Kokam's Superior Lithium Polymer Batteries. The module consists of a number of unit-cells connected in series. Kokam's module design features unit-cell cartridge construction that enables convenient maintenance. The unit-cells can be easily disassembled for repair, and this compact design results in a smaller footprint for the overall system. The modules are also designed with vent holes to allow efficient air circulation for cooling, enabling operation of up to 4 C-rate discharge. Each module is also equipped with a module BMS to monitor battery health and status at the cell level.

70

Figure A.2: Datasheet for the Kokam Lithium Ion battery (1 of 5)

Kokam's High Power Module utilizes an active cooling method via highly efficient heat dissipation technology (installation of air cooling fans and ventilation system) on every module to maintain optimal operation conditions from excessive environmental heat or heat generated from high power usage. Via active cooling, the system can continue its operation while maximizing the life of the battery.

■ **Proposed Module:**

Model	Description
KBM255-H	2P20S Kokam High Power Battery Module (KBM) 255P
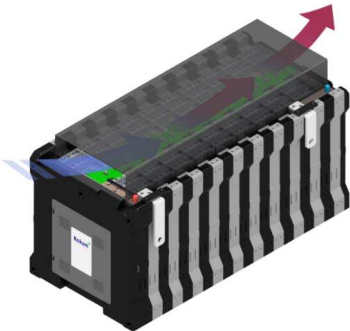
Figure 6. Module Images

Description	Value	Remark
Model Number	KBM255P-2P20S-HP-75-111	
Cell	SLPB	75Ah UHP cell
Module Configuration	2P20S	2 cell connected in parallel to form a unit cell and 20 unit cells connected in series to form a module.
Total Embedded Capacity	11.1 kWh	
Rated Capacity	10.4 kWh	0.5P-rate operation
Weight	Approx. 95	kg
Certification	UN 38.3	

71

Figure A.2: Datasheet for the Kokam Lithium Ion battery (2 of 5)

3.4 Rack

Figure 7.   Kokam 133 kWh Rack[1]   **Figure 8.   Safety Protection System**[1]

The design of the Kokam racks enables operation even in extreme conditions. They are well-suited for demanding applications such as frequency regulation and ramp rate control. Kokam racks include 5 levels of safety protection system; fuse, breaker, contactor, emergency stop switch, and enclosure with fire suppression system (shown in **Figure 10**). Multiple emergency safety procedures are augmented to enhance safety from almost all emergency situations.

■ **Proposed Rack:**

Model	Description
KRI-H-133	Kokam Rack Indoor(KRI) with 133 kWh of embedded energy
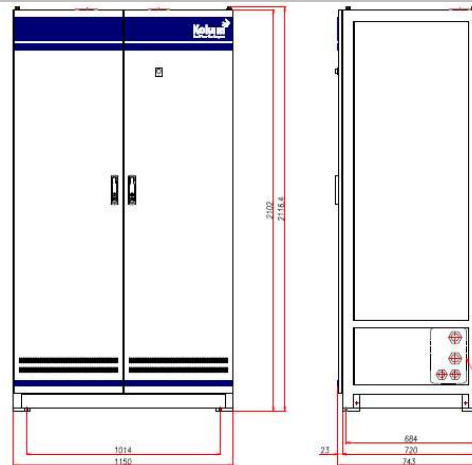
Figure 9.   Mechanical Layout [1]

---

[1] This drawing is for reference only. Actual product may be different

Figure A.2: Datasheet for the Kokam Lithium Ion battery (3 of 5)

Description	Requirement	Remarks
Model Number	KRI-H-133-H3V4-12M	Indoor rack
Total Embedded Capacity,	133 kWh	
Rated Capacity	125 kWh	1.0P-rate discharge/charge
Maximum Power Output	523 kW	*4P-rate*
Product dimension (mm)	W1,170 x D728 x H2,241.5	
Weight	Approx. 1,535 kg	

The KRI-H-133 Rack includes:

- Kokam Standard Rack (1 ea)
- KBM 255255P Module (12 ea)
- Rack BMS (1 ea)
- Module BMS (12 ea)
- Battery Protection Unit (BPU)[2] (1 ea)
- SLPB_75Ah Cell (480 ea)
- Fire Suppression System
- Cooling Fan

3.5 System
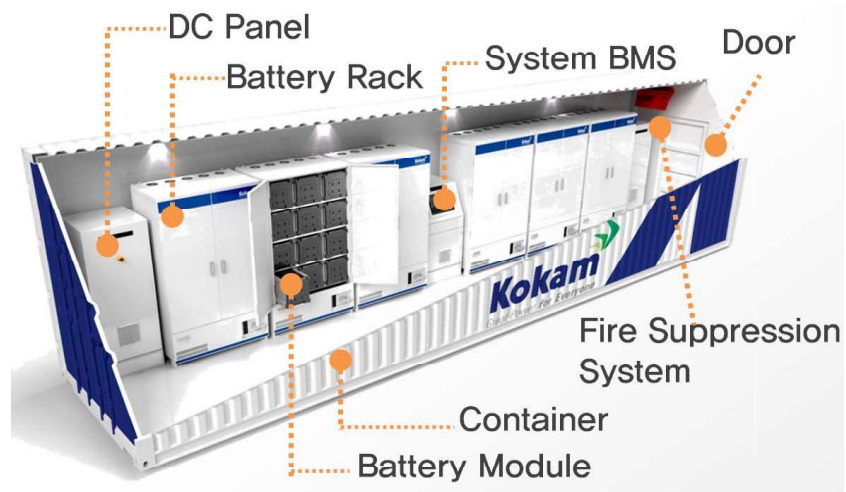
Figure 14. System Configuration (15 minute)

---

[1] This drawing is for reference only. Actual product may be different

[2] The Battery Protection Unit refers to all the electrical components, including the Master BMS, Sub MCCB etc. which are equipped within each Rack.

73

Figure A.2: Datasheet for the Kokam Lithium Ion battery (4 of 5)

Kokam Rack Indoor System (KRIS) is utilized for various applications such as peak shaving, frequency regulation, renewable energy integration, Micro-grids and UPS. Due to the high energy density of Kokam's SLPB, the KCE can store more energy in a given area than any of our competitors.

Kokam Containerized ESS(KCE) Features

- Convenient access to control circuit / Easy maintenance
- Smart Battery Management System prevents accidental failure due to misuse
- Scalable and modular design
- Interchangeable and robust standard battery modules
- Factory programmable thresholds for application specific settings(BMS)
- Remote Battery Monitoring System (Ethernet Communication)
- State-of-the-art fire detection and suppression system
- HVAC unit to maintain optimal operating conditions

■ **Proposed System:**

Description	Requirement	Remarks
System Configuration	12 racks / 4 DCP / 2 SBP	40 ft container
Total Embedded Capacity,	1,598 kWh	
Rated Capacity	1,502 kWh	0.5P-rate discharge/charge
Maximum Power Output	4 MW	*4P-rate*
Nominal Voltage	888 V_{DC}	
Min. Voltage	768 V_{DC}	
Max. Voltage	998 V_{DC}	
Round Trip Efficiency (BOL)	>95 %	

The KCE-1600 System includes:

- 40 ft. Container (1 ea)
- Kokam Standard Rack (12 ea)
- KBM 255255P Module (144 ea)
- DC Panel (4 ea)
- System BMS Panel (2 ea)
- Rack BMS (12 ea)
- Module BMS (144 ea)
- Battery Protection Unit (BPU)[3] (12 ea)
- SLPB_75Ah Cell (5,760 ea)
- Fire Detection / Suppression System
- HVAC System

Figure A.2: Datasheet for the Kokam Lithium Ion battery (5 of 5)

Model: **C2000 N5C**
Frequency: **50 Hz**
Fuel Type: **Natural Gas MI 73 +**
Emissions Performance NOx: **500 mg/Nm^3 (1.0 g/hp-h)**
LT Water Inlet Temperature: **40°C (104°F)**
HT Water Outlet Temp: **92°C (198°F)**

**Generator set data sheet
2000 kW continuous**

Our energy working for you.™

Power Generation

Measured Sound Performance Data Sheet:	MSP-1039
Prototype Test Summary Data:	PTS-269
Remote Radiator Cooling Outline:	0500-5095

Fuel Consumption (ISO3046/1)

	See Note	100% of Rated Load	90% of Rated Load	75% of Rated Load	50% of Rated Load
Fuel Consumption (LHV) ISO3046/1, kW (MMBTU/hr)	2,4,6,7	4892 (16.71)	4468 (15.26)	3793 (12.95)	2738 (9.35)
Mechanical Efficiency ISO3046/1, percent	2,4,7	42.1%	41.5%	40.8%	37.7%
Electrical Efficiency ISO3046/1, percent	2,4,6,7	40.9%	40.3%	39.5%	36.5%

Engine

Engine Manufacturer	Cummins
Engine Model	QSV91G
Configuration	V18
Displacement, L (cu.in)	91.6 (5591)
Aspiration	Turbocharged (1)
Gross Engine Power Output, kWm (hp)	2066 (2769)
BMEP, bar (psi)	18.3 (265)
Bore, mm (in)	180 (7.09)
Stroke, mm (in)	200 (7.87)
Rated Speed, rpm	1500
Piston Speed, m/s (ft/min)	10 (1968)
Compression Ratio	12.5:1
Lube Oil Capacity, L (qt)	550 (581)
Overspeed Limit, rpm	1800
Full Load Lubricating oil consumption, g/kWe-hr (g/hp-hr)	0.4 (0.3)

Fuel

Gas supply pressure to engine inlet, bar (psi)[7]	0.2 (2.9)
Minimum Methane Index	73

Starting System(s)

Electric starter voltage, volts	24
Minimum battery capacity @ 40 deg.C (104 deg.F), AH	780
Air Starter Pressure, barg (psig)	10.3 (150)
Air Starter Flow Nm^3/s (scfm)	0.37 (780)

Genset Dimensions (see note 1)

Genset Length, m (ft)	6.07 (19.9)
Genset Width, m (ft)	2.16 (7.1)
Genset Height, m (ft)	2.78 (9.1)
Genset Weight (wet), kg (lbs)	20477 (45,144)

Figure A.3: Datasheet for the Cummins QSV91G C2000 gas generator (1 of 4)

	See Notes	100% of Rated Load	90% of Rated Load	75% of Rated Load	50% of Rated Load
Energy Data					
Continuous Generator Electrical Output kWe @ 1.0 pf	6,10	2000	1800	1500	1000
Heat Dissipated in Lube Oil Cooler, kW (MMBTU/h)	5	264 (0.90)	266 (0.91)	229 (0.78)	189 (0.64)
Heat Dissipated in Block, kW (MMBTU/h)	5	490 (1.67)	494 (1.69)	425 (1.45)	364 (1.24)
Total Heat Rejected in LT Circuit, kW (MMBTU/h)	5	231 (0.79)	205 (0.70)	178 (0.61)	133 (0.45)
Total Heat Rejected in HT Circuit, kW (MMBTU/h)	5	1066 (3.64)	1011 (3.45)	818 (2.79)	584 (1.99)
Unburnt, kW (MMBTU/h)	13	108 (0.37)	100 (0.34)	90 (0.31)	64 (0.22)
Heat Radiated to Ambient, kW (MMBTU/h)	13	316 (1.08)	288 (0.98)	243 (0.83)	173 (0.59)
Available Exhaust heat to 105C, kW (MMBTU/h)	5	1263 (4.31)	1171 (3.99)	1030 (3.51)	806 (2.75)
Intake Air Flow					
Intake Air Flow Mass, kg/s (lb/hr)	4	3.12 (24687)	2.78 (22039)	2.36 (18688)	1.68 (13287)
Intake Air Flow Volume, m3/s @ 0°C (scfm)	4	2.41 (5383)	2.15 (4806)	1.82 (4075)	1.30 (2897)
Maximum Air Cleaner Restriction, mmHG (in H_2O)		22.07 (11.8)	22.07 (11.8)	22.07 (11.8)	22.07 (11.8)
Exhaust Air Flow					
Exhaust Gas Flow Mass, kg/s (lb/hr)	4	3.23 (25576)	2.88 (22847)	2.45 (19374)	1.74 (13793)
Exhaust Gas Flow Volume, m3/s (cfm)	4	6.72 (14223)	6.10 (12913)	5.27 (11154)	3.97 (8404)
Exhaust Temperature After Turbine, ^{o}C (^{o}F)	2,6	462 (863)	474 (884)	487 (909)	532 (989)
Max Exhaust System Back Pressure, mmHG (in H_2O)	6,14	37.3 (20.0)			
Min Exhaust System Back Pressure, mmHG (in H_2O)	6,14	18.7 (10.0)			
HT Cooling Circuit					
HT Circuit Engine Coolant Volume, l (gal)		424 (112)	424 (112)	424 (112)	424 (112)
HT Coolant Flow @ Max Ext Restriction, m^3/h (gal/min)		70 (308)	70 (308)	70 (308)	70 (308)
Maximum HT Engine Coolant Inlet Temp, ^{o}C (^{o}F)	8	75 (167)	75 (167)	75 (167)	75 (167)
HT Coolant Outlet Temp, ^{o}C (^{o}F)	8	92 (198)	92 (198)	92 (198)	92 (198)
Max Pressure Drop in External HT Circuit, bar (psig)		1.5 (22)	1.5 (22)	1.5 (22)	1.5 (22)
HT Circuit Maximum Pressure, bar (psig)		6.0 (87)	6.0 (87)	6.0 (87)	6.0 (87)
Minimum Static Head, bar (psig)		0.5 (7)	0.5 (7)	0.5 (7)	0.5 (7)
LT Cooling Circuit					
LT Circuit Engine Coolant Volume, l (gal)		295 (78)	295 (78)	295 (78)	295 (78)
LT Coolant Flow @ Max Ext Restriction, m^3/h (gal/min)		50 (220)	50 (220)	50 (220)	50 (220)
Maximum LT Engine Coolant Inlet Temp, ^{o}C (^{o}F)	9	40 (104)	40 (104)	40 (104)	40 (104)
LT Coolant Outlet Temp, θC (^{o}F) Reference Only	9	43.8 (111)	43.4 (110)	42.9 (109)	42.2 (108)
Max Pressure Drop in External LT Circuit, bar (psig)		1.5 (22)	1.5 (22)	1.5 (22)	1.5 (22)
LT Circuit Maximum Pressure, bar (psig)		6.0 (87)	6.0 (87)	6.0 (87)	6.0 (87)
Minimum Static Head, bar (psig)		0.5 (7)	0.5 (7)	0.5 (7)	0.5 (7)
Emissions					
NO_x Emissions wet, ppm	15	167	164	174	179
NO_x Emissions, mg/Nm^3 @5% O_2 (g/hp-h)	15	493 (1.05)	480 (1.03)	504 (1.10)	509 (1.20)
THC Emissions wet, ppm	13	1360	1408	1498	1520
THC Emissions, mg/Nm^3 @5% O_2 (g/hp-h)	13	1447	1488	1577	1536
CH_4 Emissions wet, ppm	13	1133	1145	1221	1222
CH_4 Emissions, mg/Nm^3 @5% O_2 (g/hp-h)	13	1225 2.61	1230 2.63	1307 2.85	1255 2.97
NMHC Emissions wet, ppm	13	227	263	277	298
NMHC Emissions, mg/Nm^3 @5% O_2 (g/hp-h)	13	242	278	291	301
CO Emissions (dry), ppm	13	578	575	571	584
CO Emissions, mg/Nm^3 @5% O_2 (g/hp-h)	13	965 (2.05)	953 (2.04)	943 (2.06)	922 (2.18)
O2 Emissions (dry), percent	13	9.0	8.9	8.9	8.3
Particulates PM10, g/hp-h	13	<0.06	n/a	n/a	n/a

Figure A.3: Datasheet for the Cummins QSV91G C2000 gas generator (2 of 4)

Genset De-rating

Altitude and Temperature Derate Multiplication Factor

Table A*

Derate Multiplier with Grid Parallel Operation

In Hg	mbar	Feet	Meters	20	25	30	35	40	45	50	55	60
20.7	701	9843	3000	0.75	0.75							
21.4	723	9022	2750	0.80	0.80							
22.1	747	8202	2500	0.85	0.85	0.75						
22.8	771	7382	2250	0.90	0.90	0.80						
23.5	795	6562	2000	0.95	0.95	0.85	0.75					
24.3	820	5741	1750	1.00	1.00	0.90	0.80					
25.0	846	4921	1500	1.00	1.00	0.95	0.85	0.75				
25.8	872	4101	1250	1.00	1.00	1.00	0.90	0.80				
26.6	899	3281	1000	1.00	1.00	1.00	0.95	0.85	0.75			
27.4	926	2461	750	1.00	1.00	1.00	1.00	0.90	0.80			
28.3	954	1640	500	1.00	1.00	1.00	1.00	0.95	0.85			
29.1	983	820	250	1.00	1.00	1.00	1.00	1.00	0.90			
29.5	995	492	150	1.00	1.00	1.00	1.00	1.00	1.00	0.75		
30.0	1012	0	0	1.00	1.00	1.00	1.00	1.00	1.00	0.75		
			°C	20	25	30	35	40	45	50	55	60
			°F	68	77	86	95	104	113	122	131	140
			Air Filter Inlet Temperature									

Barometer | **Altitude** (In Hg, mbar, Feet, Meters)

* Based on SAE standard ambient pressure vs. altitude. Assumes LT return temperature is 10C above air filter inlet.

Heat Rejection Factor (altitude and ambient) for HT and LT Circuits

Table C

Multiplier for HT & LT Heat Rejection vs Alt & Temp.

In Hg	mbar	Feet	Meters	20	25	30	35	40	45	50	55	60
20.7	701	9843	3000	1.11	1.13	1.14	1.15	1.17	1.18	1.19	1.20	1.22
21.4	723	9022	2750	1.10	1.12	1.13	1.14	1.15	1.17	1.18	1.19	1.21
22.1	747	8202	2500	1.09	1.10	1.12	1.13	1.14	1.16	1.17	1.18	1.20
22.8	771	7382	2250	1.08	1.09	1.11	1.12	1.13	1.14	1.16	1.17	1.18
23.5	795	6562	2000	1.07	1.08	1.09	1.11	1.12	1.13	1.15	1.16	1.17
24.3	820	5741	1750	1.06	1.07	1.08	1.10	1.11	1.12	1.14	1.15	1.16
25.0	846	4921	1500	1.05	1.06	1.07	1.09	1.10	1.12	1.14	1.15	
25.8	872	4101	1250	1.04	1.05	1.06	1.07	1.09	1.10	1.11	1.13	1.14
26.6	899	3281	1000	1.02	1.04	1.05	1.06	1.08	1.09	1.10	1.12	1.13
27.4	926	2461	750	1.01	1.03	1.04	1.05	1.06	1.08	1.09	1.10	1.12
28.3	954	1640	500	1.00	1.02	1.03	1.04	1.05	1.07	1.08	1.09	1.11
29.1	983	820	250	0.99	1.00	1.02	1.03	1.04	1.06	1.07	1.08	1.10
29.5	995	492	150	0.99	1.00	1.01	1.03	1.04	1.05	1.06	1.08	1.09
30.0	1012	0	0	0.98	0.99	1.01	1.02	1.03	1.05	1.06	1.07	1.08
			°C	20	25	30	35	40	45	50	55	60
			°F	68	77	86	95	104	113	122	131	140
			Air Filter Inlet Temperature									

Barometer | **Altitude** (In Hg, mbar, Feet, Meters)

Methane Number Capability

Load (Percent of Rated)			
100%	90%	75%	50%
73	67	n/a	n/a

Temperature & Altitude Derate

1. Determine derate multiplier vs. temperature and altitude in Table A or B depending upon your operating condition.

2. Assumes the LT return temperature is 10 deg C above the air filter inlet with a maximum LT temperature of 40 deg C.

3. If the LT temperature exceeds 40 deg C, consult factory for recommendations.

4. Altitude is based upon SAE standard ambient pressure vs. altitude. For low barometric conditions add 150m (500 ft) to site altitude.

LT & HT Circuit Heat Rejection Calculation

1. Determine derate multiplier vs. temperature derate per above.

2. Using the multiplier from #1 above as the percent load factor determine the Heat rejection from the previous page.

3. From Table C find the HT and LT circuit multiplier.

4. Multiply the result of step 2 by the result of step 3 to obtain the heat rejection at your altitude and temperature.

Specifications May Change Without Notice

Figure A.3: Datasheet for the Cummins QSV91G C2000 gas generator (3 of 4)

Alternator Data

Voltage Range	Connection Configuration	Temp Rise Degrees C	Duty[11] Cycle	Single Phase Factor	Alternator Data Sheet
380-440	Wye, 3 Phase	105	C	N/A	Note 16
400-415	Wye, 3 Phase	105	C	N/A	Note 16
3300	Wye, 3 Phase	80/105	C	N/A	Note 16
6600	Wye, 3 Phase	80C/105	C	N/A	Note 16
6300-6600	Wye, 3 Phase	105	C	N/A	Note 16
10000	Wye, 3 Phase	80/105	C	N/A	Note 16
10.5-11.0 kV	Wye, 3 Phase	105	C	N/A	Note 16
11000	Wye, 3 Phase	80/105	C	N/A	Note 16
13200	Wye, 3 Phase	105	C	N/A	Note 16

Continuous Rating Definition

Applicable for supplying power continuously to a constant load up to the full output rating for unlimited hours. No sustained overload capability is available for this rating. Consult authorized distributor for rating. (Equivalent to Continuous Power in accordance with ISO8528, ISO3046, AS2789, DIN6271, and BS5514).

Notes

1) Weights and set dimesions represent a generator set with its standard features only. See outline drawing for other configurations.

2) At ISO3046 reference conditions, altitude 1013 mbar (30in Hg), air inlet temperature 25°C (77°F)

3) Nominal performance ± 2 1/2%.

4) According to ISO 3046/I with fuel consumption tolerance of +5% -0%

5) Production variation/tolerance ±5%.

6) At electrical output of 1.0 Power Factor, 97% alternator efficiency.

7) Tested using pipeline natural gas with LHV of 33.44mJ/Nm3 (905BTU/ft3)

8) Outlet temperature controlled by thermostat. Inlet temperature for reference only.

9) Inlet temperature controlled by thermostat, outlet temperature for reference only.

10) With engine driven coolant pump.

11) Standby (S), Prime (P), Continuous (C)

12) Maximum rated starting kVA that results in minimum of 90% of rated sustained voltage during starting.

13) Tolerance +/- 15%

14) Exhaust system back pressure is a rated load and will decrease at lower loads.

15) Tolerance ±10%

16) Alternator model and data sheet information available on www.powersuite.cummins.com

Power Generation

Figure A.3: Datasheet for the Cummins QSV91G C2000 gas generator (4 of 4)

Appendix B: Raw Data

B.1 U.K. Gas Price History

B.2 U.K. Future Electricity Price Predictions

B.3 U.K. National Grid: 2016 Accepted Tender Offers
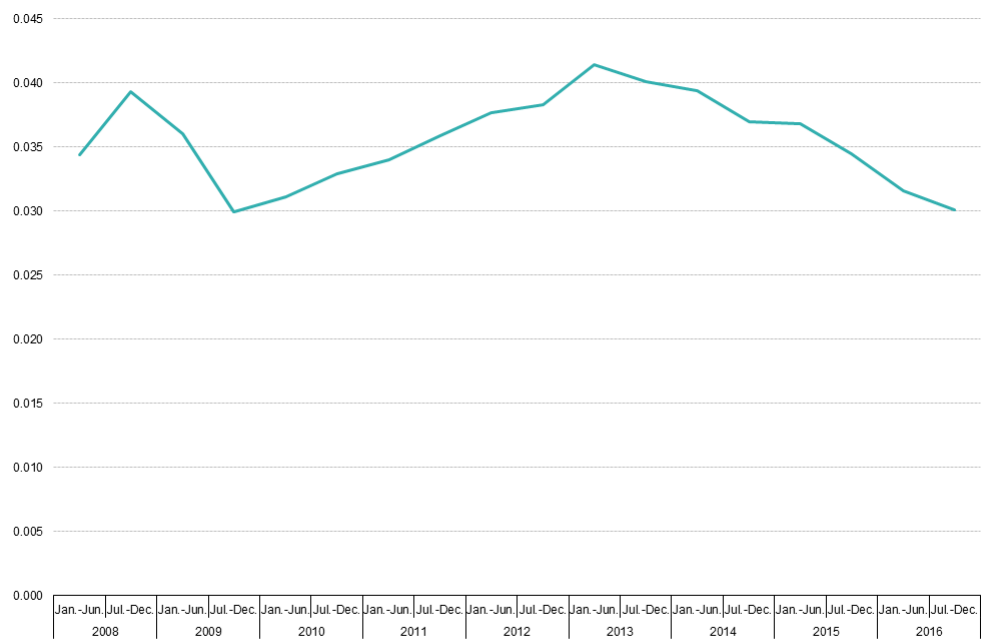
Note: annual consumption: 10 000 GJ < consumption < 100 000 GJ. Excluding VAT.
Source: Eurostat (online data code: nrg_pc_203)

Figure B.1: Graph depicting the past eight years of natural gas prices in the
United Kingdom. Note: Units for the vertical axis are EUR/kWh

Prices: wholesale prices[1,2]
Various units (2016 prices)

	units	2011	2012	2013	2014	2015
Electricity[3]	p/kWh	5.2	4.9	5.4	4.4	4.2
Natural gas	p/therm	56.2	59.6	67.9	49.9	42.6
	units	2016	2017	2018	2019	2020
Electricity[3]	p/kWh	4.2	4.6	4.7	4.8	5.1
Natural gas	p/therm	37.0	44.0	46.0	48.0	50.0
	units	2021	2022	2023	2024	2025
Electricity[3]	p/kWh	5.4	5.6	6.0	6.5	6.4
Natural gas	p/therm	52.0	55.0	57.0	59.0	61.0
	units	2026	2027	2028	2029	2030
Electricity[3]	p/kWh	5.9	6.2	5.9	5.5	6.0
Natural gas	p/therm	63.0	65.0	68.0	70.0	72.0

Notes

[1] Historical prices to 2009 for gas are from the BP Statistical Review of World Energy (http://www.bp.com/en/global/corporate/about-bp/energy-economics/statistical-review-of-world-energy.html).

They are converted to constant prices using the deflator series from the Office for Budget Responsibility (OBR): economic and fiscal outlook November 2016; table 3.7 (2016 to 2021); with supplementary note on long-term economic determinants (2022 onwards).

Where currency exchange is required, historical exchange rates (to 2015) are from the Bank of England annual average spot exchange rate (series XUAAUSS and XUAAERS). The 2015 rates are projected forwards as constant, to 2035.

Historical prices from 2010-15 for gas are converted from Argus, Bloomberg and CIF ARA Spot Price data respectively.

[2] Projected prices for gas are from BEIS's fossil fuel price projections of 2016 (https://www.gov.uk/government/collections/fossil-fuel-price-projections). There are three different scenarios (low, central/reference and high) which reflect a combination of assumptions about global fossil fuel prices and assumptions about the operation of the northern European wholesale market in which the UK buys its fossil fuels.

BEIS electricity demand projections. The demand is then re-calculated based on this price and the process repeats. This is continued until the price and demand converge to a pre-defined tolerance level.

[3] Projected electricity prices are based on DDM modelling and are scenario dependent.

81

Figure B.2: Chart displaying the predicted electricity and natural gas prices for the United Kingdom from now until 2030

| # Mnths | Tendered Frames per Service Day | | | | | | Tendered Prices | | Primary Resp. (max.) @ 0.5Hz (MW) | Secondary Resp. (max.) @ 0.5/0.5Hz (MW) |
| | Working Days (Mon-Fri) | | Saturdays | | Sundays/Bank Holidays | | Availability Fee (£/h) | Nomination Fee (£/h) | | |
	Start Time	Duration (h)	Start Time	Duration (h)	Start Time	Duration (h)				
1	2300	24	2300	24	2300	24	340	0	8	20
4	2000	20	2300	24	2300	24	340	0	8	20
8	2300	24	2300	24	2300	24	340	0	8	20
4	2000	20	2300	24	2300	24	340	0	8	20
7	2300	24	2300	24	2300	24	340	0	8	20
4	00h00	24	00h00	24	00h00	24	165	0	15	22
1	2300	24	2300	24	2300	24	2593	0	104	140
1	0000	24	0000	24	0000	24	946	131	58	60
3	2300	24	2300	24	2300	24	603	0	30	30
4	2000	20	2300	24	2300	24	603	0	30	30
8	2300	24	2300	24	2300	24	603	0	30	30
4	2000	20	2300	24	2300	24	603	0	30	30
5	00h00	24	00h00	24	00h00	24	231	0	25	33
4	2300	24	2300	24	2300	24	584	584	24	75
3	1900	21	1700	24	1700	24	201	0	10	10
8	1900	24	1700	24	1700	24	201	0	10	10
1	1900	21	1700	24	1700	24	201	0	10	10
6	2300	24	2300	24	2300	24	333	0	20	20
4	2000	20	2300	24	2300	24	333	0	20	20
8	2300	24	2300	24	2300	24	333	0	20	20
4	2000	20	2300	24	2300	24	333	0	20	20
2	2300	24	2300	24	2300	24	333	0	20	20
1	0700	16	00h00	24	00h00	24	90	0	11	15
20	00h00	24	00h00	24	00h00	24	368	0	35	46
23	6:30	16.5	7:00	16	8:00	15	1590	1590	170	170
1	0000	24	0000	24	0000	24	946	198	60	60
3	1900	21	1700	24	1700	24	190	0	6	10
8	1900	24	1700	24	1700	24	190	0	6	10
4	1900	21	1700	24	1700	24	190	0	6	10
8	1900	24	1700	24	1700	24	190	0	6	10
1	1900	21	1700	24	1700	24	190	0	6	10
1	0000	24	0000	24	0000	24	1021	198	60	60
1	0000	24	0000	24	0000	24	1199	198	60	60
1	0600	17	0700	16	0800	15	975	925	80	80
1	0600	17	0700	16	0800	15	1195	985	80	80
1	700	16	700	16	700	16	68.8	0	2	2
1	2300	8	2300	8	2300	8	167.06	0	2	2
1	700	16	700	16	700	16	91	0	2	2
6	1900	24	1700	24	1700	24	194	0	6	10
4	1900	21	1700	24	1700	24	194	0	6	10

Figure B.3: Table displaying all of the tender offers accepted by the U.K.'s National Grid in 2016.

Appendix C: Miscellaneous

C.1 Full Dispatch Strategy for BESS-Gen Configuration
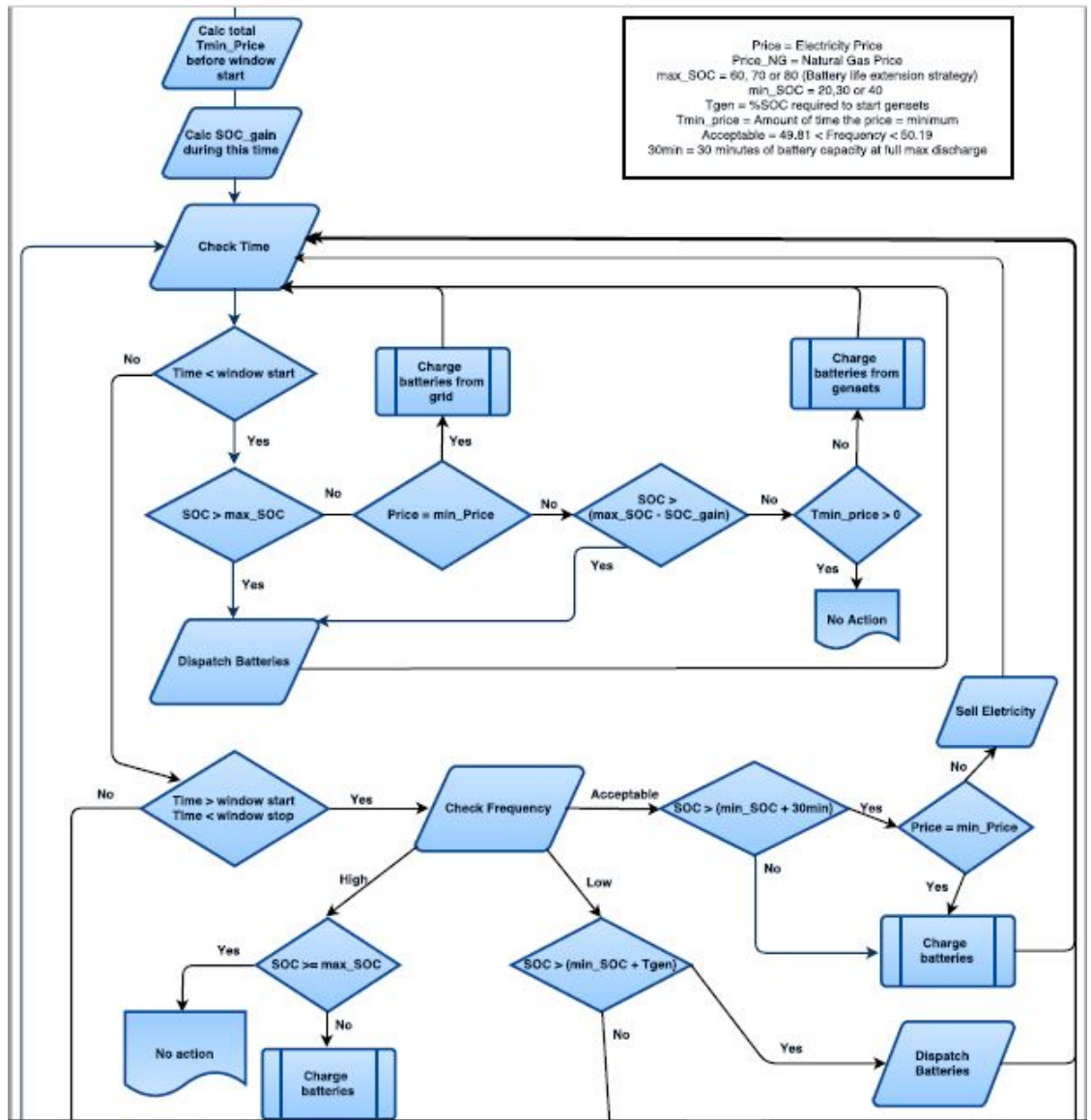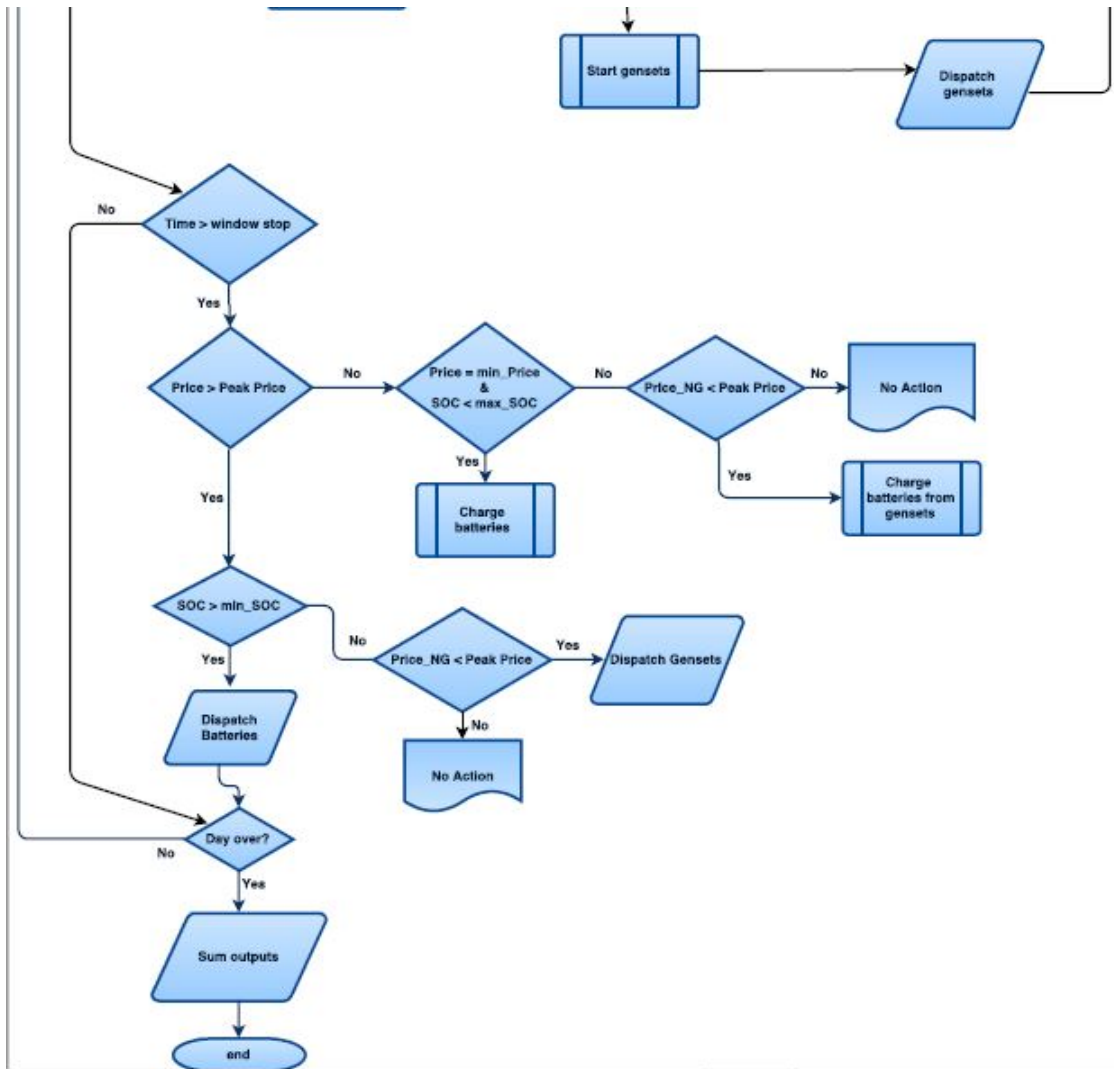
(Continued on next page)

Figure C.1: Dispatch strategy for a BESS-Gen power plant during a day in which FFR services are only offered for a fraction of the hours of the day.